Russian Chemical Reviews **84** (7) 693 – 711 (2015) © 2015 Russian Academy of Sciences and Turpion Ltd

DOI 10.1070/RCR4524

Spatial networks in solutions of wormlike aggregates: universal behaviour and molecular portraits †

A I Victorov, M A Voznesenskiy, E A Safonova

Institute of Chemistry, Saint Petersburg State University
Universitetskiy prosp. 26, Peterhof, 198504 Saint Petersburg, Russian Federation

The structures, phase behaviours and viscoelastic properties of solutions in which the growth of wormlike aggregates results in the reversible formation of a spatial network are considered. The general (independent of the molecular nature) regularities of equilibrium and dynamic characteristics of these solutions are considered and the mechanisms of manifestation of individual chemical portraits of particles are discussed. For solutions of wormlike micelles, the achievements of molecular thermodynamic theory are summarized. The potential applications of systems with controllable viscoelasticity are discussed. The bibliography includes 146 references.

Contents

I. Introduction 693
II. Branching of wormlike aggregates and phase behaviour of a spatial network 694
III. Viscoelasticity and structure of solutions containing wormlike aggregates 700
IV. Materials and devices based on micellar systems 707
V. Conclusion 708

I. Introduction

Spatial networks are formed in systems of various molecular nature. Fumed silica particles,[1] wormlike micelles of surfactants,[2] microemulsion droplets,[3,4] dipole solid spheres,[5–8] associating polymer chains [9–12] and Janus colloidal particles [13,14] can be arranged into a spatial network, thus converting the solution into a reversible physical gel.[8,15] Solutions containing gel-like particles demonstrate a diversity of viscoelastic properties and sensitivity to changes in the concentration, temperature, acidity and salinity and to external impacts.[16] The reversibility of network formation and the possibility of controlling the viscosity make these systems quite useful for a variety of applications, in particular, for decreasing the resistance to flow in heating installations,[17] for enhanced oil recovery from natural deposits,[18] for the development of paints and self-sealing protective coatings,[19] for targeted drug delivery and so on.[2]

Considerable progress has been made in the last 15 years in the studies of solutions of wormlike micelles: new experimental approaches have been developed, novel compositions were found and the scope of their application has been extended, in particular, a number of devices based on controllable aggregate growth and branching have been designed. Significant achievements were also made in the field of molecular-statistical theory and studies of kinetics, structure and thermodynamic behaviour of such systems. These objects called also giant micelles, thread-like micelles or 'living polymers' were covered in comprehensive reviews;[2,17,18,20–25] however, these publications do not sufficiently demonstrate the universal nature of some regularities inherent in the formation of a spatial network of linear aggregates. The role of molecular thermodynamic theory of aggregation [26,27] and its potential for description of the local molecular portrait responsible for the specific

A I Victorov Doctor of Chemical Sciences, Professor, Head of the Chair of Physical Chemistry at the Institute of Chemistry, SPbSU.
Telephone: +7(812)428–4059, e-mail: victorov_a@yahoo.com
Current research interests: molecular thermodynamics of fluid systems, modelling of phase equilibria and equation of state; macroscopic behaviour and 'soft' matter morphology; self-organization and nanostructures.
M A Voznesenskiy Candidate of Physical and Mathematical Sciences, Research Assistant of the same Chair.
Telephone: +7(812)428–4065,
e-mail: mikhail.voznesenskiy@gmail.com
Current research interests: Monte Carlo methods, polymer systems, general problems of static physics, theory of condensed state.
E A Safonova Candidate of Chemical Sciences, Assistant Professor of the same Chair.
Telephone: +7(812)428–4066, e-mail: e.a.safonova@spbu.ru
Current research interests: structural and thermodynamic properties of multicomponent solutions of ampliphilic compounds; aggregation, phase equlibria, distribution of dissolved components.

Received 20 October 2014
Uspekhi Khimii **84** (7) 693–711 (2015); translated by S P Svitanko

† The review continues the series of publications devoted to the development of chemistry at the Saint Petersburg State University [see *Russ. Chem. Rev.* **84** (**6**) 2015].

features of the behaviour of a particular system are not fully reflected either. This review is meant to fill these gaps.

The behaviour of solutions that differ at the microlevel but are capable of network formation shows remarkable similarity. It is manifested in systems in which particles stick together to form aggregates, which exhibit strong tendency for linear growth but can also branch. The thermodynamic behaviour of these systems are controlled by the statistical balance between ends and branching points (junctions) of the monomer chain.[8] In these systems, the effective attraction of particles resulting in phase separation is of entropic nature.

The specific microscopic portrait of the considered systems is described by molecular thermodynamic models of the aggregate free energy, which allow estimating of the free energies of branching points, ends and linear segments of the aggregate from molecular characteristics.[28] Models of this type were derived for a solution of patchy spheres,[13,29] for cross-linking polymer chains [30] and wormlike surfactant micelles.[31–33] The present paper describes the universal mechanism that controls the behaviour of reversible spatial networks of linear aggregates, gives interpretation of rheological experimental data and briefly analyzes the molecular thermodynamic models. The results obtained for polymeric and micellar reversible networks are discussed. Particular attention is given to the description of the effect of ion nature on the growth and branching of wormlike micelles of ionic surfactants.[34] In particular, for viscoelastic solutions of wormlike ionic micelles, the substantial effect of the co-ion nature on the position of the viscosity peak, which is observed upon increase in the concentration of the salt added to the solution, was elucidated.[35]

The wormlike (*i.e.*, fairly flexible) aggregates are able to diffuse in the solution with wriggling and entangling. The interchain orientational correlations can be neglected in the description of the system. Direct inter-aggregate interactions are reduced to the excluded volume effects and to possible sticking together of monomer units of different chains giving rise to branching points. In the system with branching points, collective attractive forces between the chain monomers additionally arise.[8] The structure and properties of a single wormlike aggregate (first of all, flexibility, effective excluded volume of the monomers and characteristic lifetime) determine the molecular portrait of the system. Below we demonstrate the applicability of this approach to a broad range of systems. An exception is provided by systems in which the crucial role is played by large-scale orientational ordering effects, for example, liquid-crystalline ones. This paper does not concern glass-like gels [14,36] or systems in which unstable ordered structures arise upon shear deformations. The modern reviews and monographs perfectly cover this vigorously developing area of non-linear rheology.[23,24,37–40]

The concept of entropic networks and the equilibrium properties of solutions of wormlike aggregates as well as their structural transformations and phase behaviours are considered in Section II. Section III is devoted to kinetic characteristics of the spatial network. The correlation of structural network parameters with the data of rheological experiments is discussed. The mechanisms of action of the factors that are used to control the system viscoelasticity (content of the surfactant, concentration and nature of the salt, addition of the second surfactant, *etc.*) are considered in relation to solutions of wormlike micelles. Section IV gives examples of practical application of wormlike micelle systems; good prospects of using such systems for engineering are noted.

II. Branching of wormlike aggregates and phase behaviour of a spatial network

II.1. Entropic networks

In the systems containing branched aggregates and spatial networks, phase separation often takes place. Typical examples are micellar solutions and microemulsions.[41,42] Phase separation can be induced by addition of a salt or change in the temperature, surfactant concentration or solvent composition. The equilibrium phases can contain relatively dense or dilute aggregate networks. The network of branched wormlike micelles can be detected by cryogenic transmission electron microscopy (cryo-TEM) in water-enriched mixtures pentaethylene glycol monodecyl ether + water + n-octane near the two-phase boundary.[42] Similar phase behaviour and morphology are observed in various systems comprising not only wormlike surfactant micelles or microemulsions but also, for example, dilute dispersions of dipole particles.[28] The similarity of the behaviours of self-organized linear chains in different systems is explained in terms of the concept of entropic networks.[8,28]

A linear chain can be composed of various structural elements (solid sphere bearing a dipole, colloidal particle with surface sites capable of specific interactions or amphiphilic molecules forming a wormlike micelle); however, in all cases, aggregation of structural elements to form a linear chain is energetically favourable.[8,28] Linear aggregates have a finite size, because the presence of chain ends (a sort of defects) increases the entropy of the system. Another possible type of defect is the branching point of the linear chain. Both types of topological defects have higher energy than an element of an infinite linear chain. Nevertheless, both defects increase entropy; therefore, they exist at any finite temperature of the system.[8,28] If the energy of chain ends is higher than the energy of branching points, the latter start to predominate at rather low temperature, and the system is organized into a large-scale branched spatial network.

The simplest theory of entropic networks was proposed by Tlusty and Safran.[8] In the mean force field approximation, the volume fraction of chains φ (roughly equal to the total volume fraction of surfactant molecules if the chain is a wormlike micelle) is proportional to ψ^2, where $\psi(\vec{r})$ is the probability that the chain fragment ends in point $\vec{r}$.[43] Then for the concentration (partial density) of chain ends, one has

$$\rho_e \sim \psi \exp\left(-\frac{\varepsilon_e}{T}\right) \sim \varphi^{1/2} \exp\left(-\frac{\varepsilon_e}{T}\right) \quad (1)$$

where the Boltzmann factor takes into account the energy of defect formation ε_e. Similarly, for branching points (values with the subscript j meaning junction) in which ends of three linear chains meet, one gets

$$\rho_j \sim \psi^3 \exp\left(-\frac{\varepsilon_j}{T}\right) \sim \varphi^{3/2} \exp\left(-\frac{\varepsilon_j}{T}\right) \quad (2)$$

Considering the system as a gas of non-interacting defects, by minimizing the free energy of the system

$$f = k_B(T\rho_d[\ln\rho_d - 1] + \varepsilon_d\rho_d)$$

where ρ_d and ε_d are the density and the energy of defects, respectively, one finds that defect of any type (end or junction) makes the same contribution to the system free energy

$$f_{min} = -k_B T \rho_d$$

Thus, the equation of the free energy of an equilibrium system of branching linear chains can be written in the form

$$\frac{f}{k_B T} = -\rho_e - \rho_j + \frac{\varphi^2}{2} \quad (3)$$

in which the last term accounts for excluded volume of the chain.

The equation for osmotic pressure derived using Eqns (1) and (2) for the density of defects,[8]

$$P = \varphi^2 \frac{\partial(f/\varphi)}{\partial\varphi} = \frac{\rho_e - \rho_j}{2} + \frac{\varphi^2}{2} \quad (4)$$

has a negative term, indicating the presence of attractive forces in the system. Equation (4) has contributions related to the defect topology: the contribution of repulsion caused by the chain ends and the contribution of attraction caused by the presence of junctions. These contributions describe the average effective forces of interaction between all chain fragments arising in the macroscopic system in the presence of defects rather than microscopic forces of interaction between the defects (this simple model assumes that defects do not interact). When attraction becomes sufficiently strong, phase separation takes place. According to the model in question, this occurs below the critical temperature

$$T_c \sim \varepsilon_e - 3\varepsilon_j \quad (5)$$

Phase separation is similar to separation of a fluid containing a mixture of junctions and ends. In a lower density phase, there are more ends than junctions, whereas a higher density phase is dominated by junctions. The translational entropy of the chains decreases in the more dense phase; nevertheless, the total entropy of the system increases due to increase in the junction density.

The chain junctions and ends are thermal defects. On cooling the system, the densities of these defects exponentially decrease [see Eqns (1) and (2)], resulting in longer branches. The junctions disappear more slowly because of lower energy compared to the chain energy. As the system is cooled below the critical temperature, the two-phase area increases. However, a further decrease in the temperature shifts the equilibrium line towards very low densities.[28] The described retrograde behaviour is due to the collective properties of a solution of chains with thermal defects and is not directly related to the chemical nature, *i.e.*, the molecular 'portrait', of the system.

The entropy-controlled phase separation in a dilute solution of cross-linking chains was first theoretically predicted by Drye and Cates [44] and subsequently described by other authors for diverse systems, in particular, by computer simulation of a system of linear chains forming sticky spheres with patches responsible for specific interactions.[29] This system can serve as a simple model of a solution of specifically interacting colloidal particles or Janus micelles. The fluids composed of aggregated spheres are described by Wertheim's thermodynamic perturbation theory. The calculations according to the best known version of this theory [statistical associating fluid theory (SAFT)] [45] are consistent with the computer simulation results.[29] A typical retrograde two-phase region extending to the very low-density area is shown in Fig. 1. At low temperatures, the patchy particles with low functionality capable of associating with only few neighbours can form a spatial network of very low density, so-called empty liquid (Fig. 2).

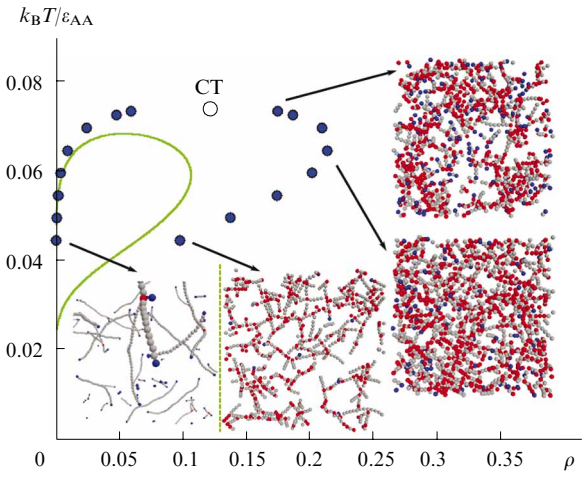


Figure 1. Phase equilibrium lines for a fluid of associating spheres with contact sites of two types A and B.[29]
Two A sites are located on the poles of each sphere, nine B sites are uniformly distributed along the equator. The A–A bonds result in sphere association to linear chains; A–B bonds give rise to junctions; B–B bonds are not considered. The energy of breaking the linear chain is designated by ε_{AA}; $\varepsilon_e = \varepsilon_{AA}/2$ is the formation energy of each of the two resulting chain ends. For junction formation, $\varepsilon_j = \varepsilon_{AA}/2 - \varepsilon_{AB}$, $\varepsilon_{AB} = 0.37\,\varepsilon_{AA}$. The points were obtained by the Monte Carlo method; (CT is the critical point). The curve (binodal) corresponds to SAFT theory calculations. The system configurations obtained in the computer experiment are shown for selected points in the phase coexistence line (arrows). The colour designates ends (blue) and junctions (red).

A similar phase behaviour of equilibrium physical gels, which are formed in solutions of associating chains of

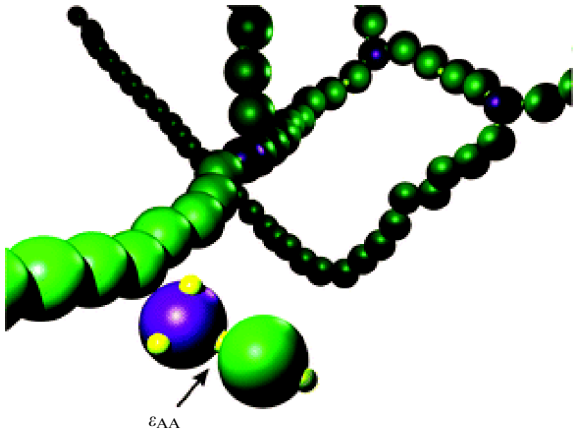


Figure 2. Low-density network in a binary mixture of particles bearing two or three identical contact sites A. Binding of two contacts decreases the energy by ε_{AA}.[13]

polymer molecules, was predicted by a simple (mean-field) theory of associating chains.[30,46,47] For these systems, relative positions of the percolation lines (formation of a macroscopic-scale spatial network) and phase boundaries were studied [30,46] and the relationship between the associating chain theory and SAFT was elucidated.[30] The classical Flory–Stockmayer criterion,[48] which determines the percolation threshold, was extended to networks with multiple types of specific bonds.[13]

Apart from the simplified views considered above, strict statistical mechanics descriptions of an ensemble of branching chains have also been developed [49–52] based on the analogy between a polymer and a magnet known from the polymer physics.[43] This description makes it possible to establish the formal relationship between the statistical sum of a solution of branching chains and the statistical sum of a Heisenberg magnet. According to the most complete version of this theory reported by Zilman and Safran,[51] chain branching can have an arbitrary functionality. The mathematics of this theory is quite complicated; however, the results in the mean-field approximation are simple. For systems with threefold functionality junctions (three linear chains meet in the branching point), the theory gives Eqns (3) and (4); the numerical coefficients in Eqns (1), (2) and (5) change but the form is retained. The volume fraction of surfactant chains in the critical point [51]

$$\varphi_c \approx \exp\frac{\varepsilon_j - \varepsilon_e}{T} \tag{6}$$

is a small quantity at a low critical temperature. The theory predicts the retrograde behaviour: above the critical temperature no phase separation takes place, while at low temperatures junctions are no longer sufficient (the defect is generated by thermal motion) to induce phase separation.

It was noted above that branching gives rise to attraction between the chain monomers and diminishes their effective excluded volume.[30,46,51] According to the Zilman–Safran theory, phase separation is possible only for systems with threefold junctions. The attraction caused by junctions of fourfold and higher functionality is not strong enough to induce phase separation. Highly branched chains can be self-assembled to a gel but if phase separation does occur in the system, it is caused by interchain interactions rather than by the entropy of junctions.

The theory predicts the average distance between the nearest chain defects. In particular, for junctions of threefold functionality, one gets [51]

$$\bar{l}_d = \frac{2\varphi l_p}{(\varphi_e + 3\varphi_j)} \tag{7}$$

where l_p is the persistence length of the chain, φ_e and φ_j are the volume fractions of the ends and junctions, respectively. In a system of non-branching chains, ends predominate. From Eqns (1) and (7), the average distance between the ends

$$\bar{l}_d \sim \varphi^{1/2}$$

i.e., the chain length increases with increase in the monomer concentration according to this power law. For highly branching chains (dominated by junctions)

$$\bar{l}_d \sim \varphi^{-1/2}$$

i.e., the average distance between junctions decreases with increase in the concentration. Thus, as the concentration increases, $\bar{l}_d$ first increases and then decreases. The maximum is located at the percolation threshold, where $\varphi_e = 3\varphi_j$. The effective radius of the largest aggregate formed by sticking (branching) chains [51]

$$\bar{R} \cong \left(\frac{2\varphi}{\varphi_e - 3\varphi_j}\right)^{1/2} l_p \tag{8}$$

becomes infinite upon percolation. For a low system density (φ), aggregates become larger but more and more dilute as the density increases. As the percolation threshold is reached, a further density increase leads to a denser network.

The Zilman–Safran theory [51] takes into account the spatial correlations of the density. It can serve to calculate the static structure factor and estimate the correlation length. Note that the characteristic correlation length can be determined by light (LS), neutron (SANS) and X-ray (SAXS) scattering techniques.

II.2. Shape and free energy of defect formation

The energies of ends and junctions depend on the microscopic characteristics and local chemical composition of the chain. If a chain is described in terms of mean-field rather than strict statistical mechanics approaches, these energies are represented by averaged characteristics — mean-force potentials and free energies.

The free energies of micellar systems can be estimated by means of either molecular thermodynamic models of aggregation [27,31,32,53,54] or phenomenological approach.[55,56] The free energies are controlled by the spontaneous curvature of the surfactant monolayer and depend on its temperature and composition. The dependence of the free energy (f_{curv}) on the curvature is expressed by the Helfrich phenomenological relation [55]

$$f_{curv} = \frac{k}{2}\left(\frac{1}{R_1} + \frac{1}{R_2} - C_0\right)^2 + \frac{\bar{k}}{R_1, R_2} \tag{9}$$

where k and $\bar{k}$ are the bending and saddle-like deformation elastic moduli, respectively, C_0 is the spontaneous curvature, *i.e.*, the curvature that is spontaneously acquired by a surfactant film in the absence of restricting external factors, and R_1 and R_2 are the local values of the principal radii of curvature.

Since Eqn (9) is the result of free energy expansion in the curvature, its applicability is restricted to small-curvature aggregates such as microemulsion droplets or coronas of large-core micelles. The free energy of an end (junction) is defined as the free energy difference between a surfactant molecule at the end (junction) and a molecule in the cylindrical part of the micelle. The energies of spherical ends (positive curvature, $R_1 = R_2$) and junctions [saddle-like curvature, $(1/R_1)(1/R_2) < 0$] are affected by fine changes in the system microscopic parameters, resulting in a change in the spontaneous curvature and elastic moduli.[57] Indeed, the replacement of the hydrocarbon solvent considerably influences the behaviour of reverse wormlike micelles formed by lecithin in the presence of water.[20] The addition of water to a solution of lecithin in isooctane causes intense

growth of wormlike aggregates, which are connected to form a gel; phase separation takes place: the gel coexists with the phase of a pure hydrocarbon. In a lecithin solution in cyclohexane, wormlike aggregates do not grow so rapidly; the formation of a gel requires that several times more water be added. Further increase in the content of water in the system results in gel destruction, disintegration of the aggregates and phase separation to give excess water coexisting with a solution of reverse spherical micelles in the hydrocarbon.

There are also other examples[58] of how the chemical individuality of the system can be manifested against the universal behaviour of an ensemble of wormlike aggregates dictated by the balance of defects (junctions and ends). An anionic surfactant, aerosol-OT, forms branched micelles in aqueous solution in the presence of an ionic liquid additive — 1-butyl-3-methylimidazolium bromide (bmimBr). When the bromide ion is replaced by BF_4^-, only spherical aggregates are formed in the system.[59] It is believed that owing to the lack of uniformity of the local content of $bmim^+$ ions in the micelle corona, packing of molecules into saddle-like aggregates is preferred, and this facilitates the formation of junctions. It is known that the nature of cations can substantially influence the aggregation of anionic surfactants. However, the mechanism of the observed pronounced effect of the surfactant co-ion present in solution remains obscure.

The fine effects being discussed cannot be quantitatively described as yet. Nevertheless, the key features of the 'molecular portrait' of aggregates can be reflected using molecular thermodynamic models. Indeed, for an aqueous solution of hexaethylene glycol monodecyl ether — a non-ionic surfactant with molecules having large polar 'heads' — percolation and phase diagram were predicted and received molecular interpretation.[56] Presumably, the dependence of free energy on temperature is determined by the change in the spontaneous curvature; the elastic moduli in expression (9) remain invariable. The temperature dependences of the free energies of junctions and ends are shown in Fig. 3. As the temperature rises, the energy of ends increases, while the energy of junctions decreases, which is caused by dehydration of the heads in the surfactant micelle corona. As this takes place, the spontaneous curvature decreases and junctions become preferred over spherical ends having higher curvature.[56] This can account for the existence of the lower critical phase separation temperature in the experimental phase diagram (Fig. 4). The Zilman–Safran theory with temperature-dependent energies of defects predicts the lower critical temperature, which is in agreement with experimental data; spatial networks are located in the high-temperature region of the diagram.

The phenomenological model of free energy [see Eqn (9)] was used to determine the equilibrium shapes of junction and end surfaces.[15,57] The found optimized shapes are presented in Fig. 5. Junctions of a similar shape can be detected by the cryo-TEM technique. The Y-shape resembles the first image of the junction proposed by Porte *et al.*:[60] a bilayered flat fragment in the central part of the junction is surrounded by toroidal elements. The junctions of such geometry can be described within the framework of molecular thermodynamic models of the free energy of aggregation of micelles formed by classical surfactants and diblock copolymers (in particular, ionic ones).[31,32,61]

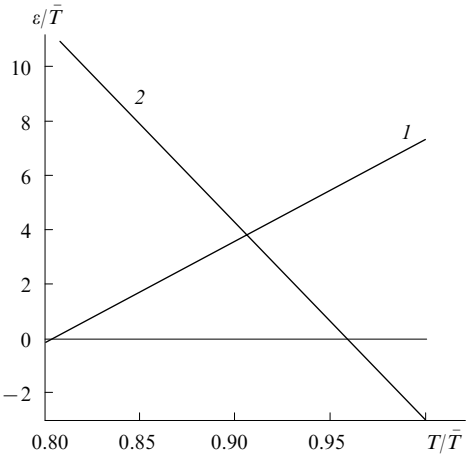


Figure 3. Temperature dependences of free energies of ends (*1*) and junctions (*2*) for non-ionic surfactant aggregates (hexaethylene glycol monododecyl ether, $C_{12}E_6$) in water.[56]
The spontaneous curvature was determined experimentally. $\bar{T}$ = 341 K is the temperature selected as the standard value.

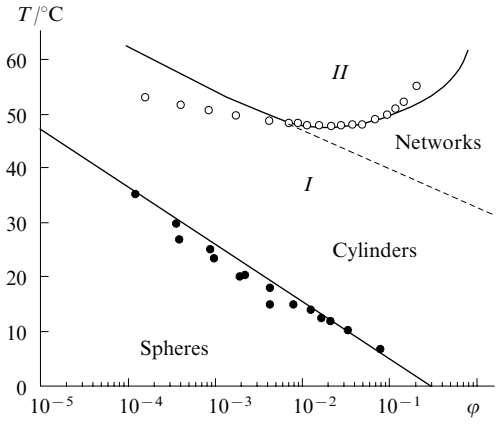


Figure 4. Temperature–surfactant volume fraction diagram for a $C_{12}E_6$ + water mixture.[56]
The dots are experimental values and the curves are calculations. Lower line: boundary of spherical to cylindrical (wormlike) aggregate transition in the single-phase region *I*; Upper line: predicted spinodal for phase separation (region *II*) into a dense network and a dilute phase (the dots show the experimental binodal); the dashed line is the predicted percolation threshold above which the network of branched micelles fills the whole solution volume.

For micellar junctions, the first molecular thermodynamic model of the free energy of aggregation was developed by May *et al.*[62] As usual for classical models, the free energy of aggregation comprises contributions described phenomenologically (contribution of the transfer of hydrophobic tails from the solution to the aggregate, work of formation of the core surface — its boundary with the environment) and contributions that depend explicitly on the molecular characteristics. The model of May *et al.* takes into account the steric repulsion between the polar heads of surfactant molecules and the contribution of the deformation of hydrocarbon tails upon packing into the micellar core. The latter value is estimated using the self-consistent

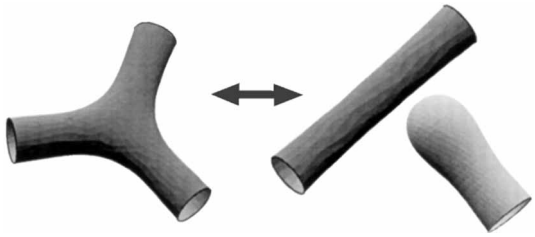


Figure 5. Junction formation upon the coalescence of the central part of a cylindrical micelle with its ends.[56]
The equilibrium form was found by numerical minimization of the free energy of curvature using triangulation technique (Evolver software). In the central part of junction, its surface is nearly flat. The cylinder ends by an expanding cap.

field theory;[63] this takes into account the core size and shape and details of the molecular architecture of the tails, in particular, rotational isomerism. However, this model has a limited applicability: within the framework of this model, junctions are always energetically less favourable than non-branched cylinders. This model also neglects the obvious dependence of the electrostatic contribution on the salinity and molecular characteristics; therefore, it is unsuitable for the description of ionic surfactant systems.

A simple expression for the electrostatic contribution to the free energy of micellar junction was obtained from the approximate analytical solution of the Linear Poisson–Boltzmann (LPB) equation for a torus.[31] The introduction of the electrostatic contribution into the classical molecular thermodynamic aggregation model[27, 53, 54] provides the possibility to describe systems of branching ionic micelles. The model shows that at high salinity, the free energy of aggregation may prove to be lower for junctions than for spherical ends. Moreover, there is a narrow concentration range in which the junctions have a lower free energy than aggregates of other shapes, which implies the system tendency to form bicontinuous structures. Further addition of the salt to the system results in stabilization of the lamellar phase.[31]

The free energies of junctions and ends calculated in terms of the molecular thermodynamic model are used as the input parameters in the Zilman–Safran theory, which can serve to predict the phase equilibria, the percolation line and other characteristics of the structure depending on the surfactant and salt concentrations.[31, 61] An example of such prediction made for an aqueous solution of erucyl bis(hydroxyethyl) methylammonium chloride (EHAC) + NaCl demonstrated that phase separation can be induced by addition of either the salt or the surfactant to the solution.[61] However, an increase in the surfactant concentration at low salt content induces only gel formation but no phase separation takes place. The addition of the salt to the resulting gel causes phase separation: the spatial network with a high concentration of junctions coexists with a sparse network with a low junction concentration (however, the percolation threshold has already been crossed). Further increase in the salt concentration destroys the denser structure, the coexisting phases becoming a sol (solution of separate aggregates) and a gel.[61]

The Zilmana–Safran theory predicts the intense branching and percolation in the situations where the energies of junctions and ends differ little[15, 57]

$$\varepsilon_e \cong \varepsilon_j$$

This fact was used to evaluate the branching conditions for micelles of a diblock copolymer with a weak polyelectrolyte chain present in the molecule. The geometry of branching of such a micelle is shown in Fig. 6. The swollen polyelectrolyte corona is sensitive to the solution acidity and salinity. The molecular thermodynamic description of this system is based on the analytical version of the self-consistent field theory,[64, 65] which has been extended to systems of aggregates having the geometry of junctions.[32] The free energy of aggregation takes into account the mixing effects in the swollen corona and the electrostatic interactions of the mobile ions that have penetrated into the corona and the dissociating groups present in the polymer chains.

The local equilibrium degree of dissociation of the polyelectrolyte is determined by free energy minimization. The expression describing the ionic contribution to the free energy of aggregation reflects the osmotic pressure of the mobile ions in the swollen corona and the entropy of distribution of the charges located on the chains at equilibrium.[32] According to this model, the size and shape of the optimal aggregate are controlled by a number of competing factors. The tendency toward decreasing the contact surface area between the hydrophobic core and the surrounding solution results in a decrease in the aggregate curvature (the surface area of the contact per surfactant molecule is reduced). The elastic response of the hydrocarbon chains prevents them from stretching, thus increasing the area per chain. The electrostatic repulsion and the excluded volume effects in the micelle corona force the chains to stretch but simultaneously they stretch the surface. The optimal aggregate shape is determined by the balance of these opposite trends, which is fairly sensitive to the molecular characteristics of the system and to external impacts.

Despite the relative simplicity of the described mean-field model, to estimate the free energy of aggregation, its numerical solution is required. It is necessary to solve the Euler–Lagrange equations to determine the equilibrium

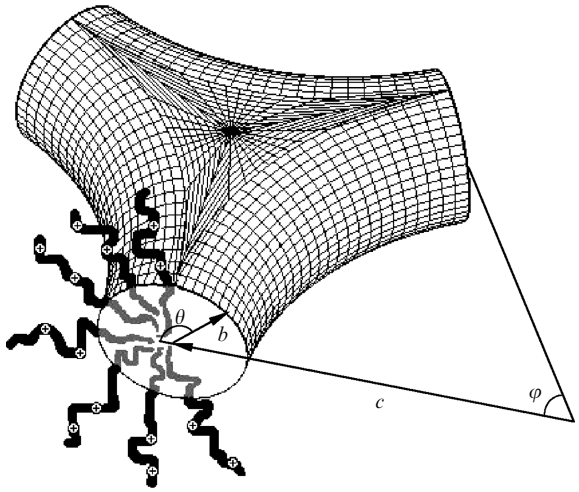


Figure 6. Geometry of the junction connecting three cylindrical micelles of an amphiphilic diblock copolymer.[32]
Chains of a weak polyacid (dark) form a corona swollen in the surrounding solution and hydrophobic non-ionic chains (light) form the aggregate core. b and c are the smaller and larger radii of the torus element, respectively; φ and θ are the angles that specify the position of a point on the torus surface.

concentration profiles of the components and the equilibrium profile of the degree of ionization of the polyelectrolyte chains in the swollen corona; the calculation also includes free energy minimization with respect to the curvature radii of the aggregates.[32]

A simpler approach to determining the optimal aggregate shape is provided by expansions of the free energy of the swollen corona in the curvature. These expansions make it possible to determine the properties of curved structures when properties of the planar structures are known and to estimate how the deformation would affect the aggregate characteristics, for example, the local degree of dissociation.[33] These expansions prove to be useful for aggregates in which the corona thickness is much less than the core radius, so-called crew-cut micelles. In this case, it is possible to derive analytical expressions for estimating the spontaneous curvature and elastic moduli[33] from molecular parameters. These expansions in combination with the classical model of the unswollen hydrocarbon core of an aggregate were used to predict the polymorph transformations. Figure 7 shows the results for a crew-cut aggregate obtained by two methods

— numerical solution using full (not expanded in the curvature) model;

— calculation based on expansions in the curvature for the free energy of the micelle corona.

The results of the two methods differ little. As expected, in the case of aggregates containing a weak polyelectrolyte,[65] a change in the salinity results in an unusual sequence of shapes for pH values of the surrounding solution close to pK_a. Pronounced tendency for branching and formation of bicontinuous structures is observed: in the light grey part of the diagram, the Y-shaped junction is the most stable structure. The polymorph transformation

$$S_1 = 1/2 \longrightarrow S_2 = 2$$

within the region of stable cylinders corresponds to the transition from branched wormlike micelles to non-branched ones.

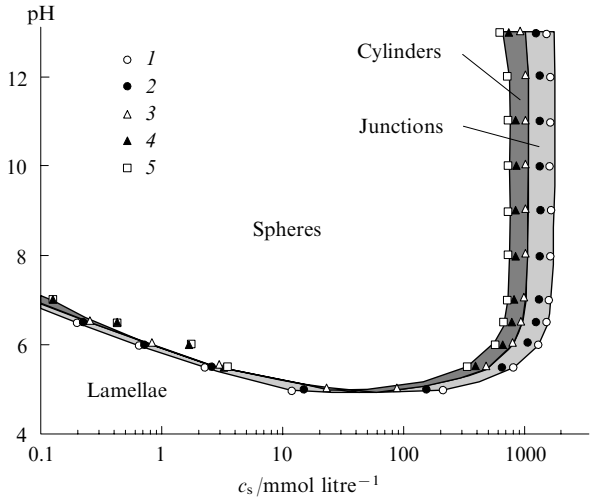


Figure 7. Predicted stability regions of aggregates of different shapes depending on pH and salinity (c_s) of the solution for a diblock copolymer formed by a hydrophobic subchain (380 monomers) and a weak polyelectrolyte subchain (20 monomers).
The coloured areas and the curves show the stability regions and lines of polymorph transformations obtained by the self-consistent field model.[32] Designations: polymorph transformations found by expansion of the free energy of the aggregate corona in the curvature.[33] $S_1 \rightarrow S_2$ implies the transformation of aggregates of morphology S_1 into aggregates of morphology S_2, where S_1, $S_2 = 0$, 1/2, 1, 2 for the plane, junction, cylinder and sphere, respectively: $0 \rightarrow 1/2$ (*1*), $0 \rightarrow 1$ (*2*), $1/2 \rightarrow 1$ (*3*), $1/2 \rightarrow 2$ (*4*), $1 \rightarrow 2$ (*5*); $pK_a = 5$ for the dissociation constant of polyelectrolyte ionic groups.

This model calculation demonstrates that branched micelles serve as intermediate structures between linear aggregates and a perforated bilayer. Indeed, as shown in Fig. 8 for an aqueous mixture of ionic and non-ionic surfactants, sodium dodecyl sulfate (SDS) + *N*-dodecyl-β-D-glucopyranoside (DDGP), this transition is actually observed in the experiment. The addition of DDGP to spherical SDS micelles induces the formation of long

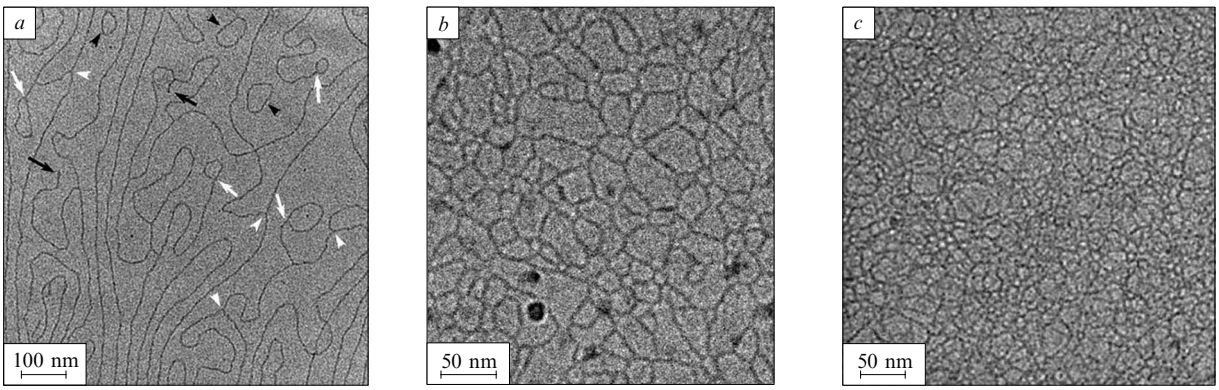


Figure 8. Branched aggregates and saturated networks for a SDS + DDGP mixture upon increase in the relative concentration of non-ionic surfactant (from *a* to *c*) at a invariable total surfactant concentration.[66]
(*a*) The system demonstrates numerous ways to avoid the formation of ends (dark long arrows) including the formation of junctions (light long arrows), short segments closed to form rings (dark short arrows) and rings connected to the aggregate body (light short arrows);
(*b*) saturated network (SDS : DDGP = 20 : 80) in which most of the junctions has threefold functionality;
(*c*) high density of junctions for the SDS content of 8 mass %; the network resembles a perforated bilayer.

branched micelles (see Fig. 8 *a*). At a higher relative content of DDGP (the total concentration of the two surfactants is constant), the density of junctions increases and a saturated network is formed (see Fig. 8 *b*,*c*).

III. Viscoelasticity and structure of solutions containing wormlike aggregates

III.1. Rheological behaviour of solutions containing entangled flexible chains

A general feature of reversible spatial networks is viscoelasticity: the ability to exhibit both fluidity and certain elasticity under the action of deformation force. The knowledge of viscoelastic characteristics, which is valuable by itself, makes it possible to draw important (although indirect) conclusions about the structure of the solution. In particular, the hypothesis that micellar aggregates can branch was first put forward based on results of rheological studies [60, 67] well before the presence of junctions was confirmed by numerous cryo-TEM data.[66] Currently, rheometry is one of the most popular methods of experimental investigations of self-assembling systems.[40]

For non-cross-linked polymers in which the spatial networks arise upon chain entanglement, the molecular mechanisms of diffusion and stress relaxation have been studied rather comprehensively.[43,68] The diffusion of polymer chains in semidilute and concentrated solutions occurs *via* snake-like motions of chains (reptations) in an effective tube formed by entanglements of surrounding chains. According to the reptation theory, the viscosity and elastic modulus variations upon changes in the average chain length and polymer concentration follow power laws.[68]

The systems of chains experiencing linear growth, in particular, solutions of wormlike micelles are similar to polydisperse polymers but with the difference that these chains continuously break and recombine. The presence of thermodynamically equilibrium distribution of chains along the length distinguishes these systems from polymers, which have invariable (frozen) polydispersity. Taking account of the concentration dependence of the equilibrium chain length in terms of the reptation theory results in the change in the power law exponents with respect to those in the same dependences for polymers. However, in the description of rheological properties of the system, the key role is played by the breaking and recombination kinetics.

Cates and co-workers [69–71] proposed that chain scission and recombination provide an additional mechanism of stress relaxation apart from reptation. If chains break frequently, numerous breakage and recombination events take place before the applied stress would relax, and the 'memory' of both the initial length and initial position of chains disappears. Therefore, relaxation of any segment of the effective tube in which chain reptation takes place occurs at the same rate and the stress relaxation of the spatial network is described by the monoexponential dependence with the characteristic time τ_r [22]

$$\tau_r = (\tau_{break}\,\tau_{rep})^{1/2}$$

where τ_{break} and τ_{rep} are the characteristic times of breaking (recombination) and reptation of chains of the average length $\bar{L}_c$.

The assumption of frequent chain scission can account for the unique rheological behaviour of solutions of wormlike micelles: despite the pronounced polydispersity, the system relaxation is usually described by an exponential law with only one relaxation time τ_r (unlike polydisperse polymers). Therefore, the rheological data for wormlike micelles in solutions can be analyzed using the Maxwell model — the simplest theoretical model of a viscoelastic system combining ideally viscous and ideally elastic elements.

For semidilute solutions of wormlike micelles in experiments at low shear rates, Newtonian flow is usually observed (Fig. 9). As a rule, the viscosity starts to decrease after some critical shear rate has been exceeded. The value reciprocal to this rate can serve as the estimate for the characteristic time of system relaxation τ_r. The clear-cut plateau allows one to estimate the viscosity at a zero shear rate (η_0); according to the Maxwell model, this value can be represented as

$$\eta_0 = G_0\tau_r \tag{10}$$

where G_0 is the shear modulus.

In the dynamic rheological experiments, the sample is subjected to oscillating shear deformations and the frequency dependences are measured for the real and imaginary parts of the relaxation modulus: the storage modulus $[G'(\omega)]$ characterizing the elastic deformation energy and the loss modulus $[G''(\omega)]$ characterizing the energy dissipation during viscous flow. The Maxwell model gives the following expressions for these quantities:

$$G'(\omega) = \frac{\omega^2\tau_r^2}{1+\omega^2\tau_r^2}G_0$$

$$G''(\omega) = \frac{\omega\tau_r}{1+\omega^2\tau_r^2}G_0$$

It can be seen that $G'(\omega)$ tends to the shear modulus G_0 in the high-frequency limit; the relaxation time is found as

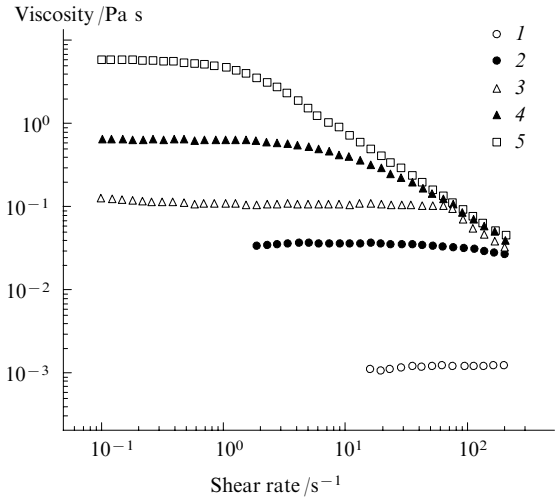


Figure 9. Dynamic viscosity *vs*. shear rate for solutions of mixed micelles of cetyltrimethylammonium bromide (CTAB) and sodium oleate (NaOL) with an invariable total amount of the surfactant (0.1 mol litre^{-1}) and mole fractions of NaOL equal to 0 (*1*), 0.2 (*2*), 0.3 (*3*), 0.23 (*4*) and 0.25 (*5*).[72]

$$\tau_r = \omega_r^{-1}$$

from the condition

$$G'(\omega_r) = G''(\omega_r) \tag{11}$$

i.e., from the frequency at which the measured moduli are equal. Hence, the viscosity at the zero shear rate can be estimated by relation (10).

If the elastic modulus does not reach a plateau at high frequency, the experimental determination of G_0 is difficult. This is related to fast relaxation mechanisms, which cannot be described by the Maxwell model (see below). The theoretical estimation of G_0 is possible based on the ratio borrowed from the theory of elasticity of polymeric spatial networks,[43]

$$G_0 = \frac{k_B T}{\xi_m^3}$$

where ξ_m is the characteristic linear dimension of the network cell (Fig. 10).

The characteristic relaxation time is conveniently estimated from the Cole–Cole plot (Fig. 11), which shows the loss modulus $G''(\omega)$ as a function of the elastic modulus $G'(\omega)$. In this plot, the Maxwell model is represented by a semicircle. The experimental data are located in the left (low-frequency) region. For the frequencies corresponding to the characteristic time of micelle breakage τ_{break}, the experimental dependences markedly deviate from the Maxwell semicircle. If chain reptation is the predominant mechanism of relaxation at times $< \tau_{break}$, the dependence of $G''(\omega)$ on $G'(\omega)$ is linear with a slope of -1.[74] At higher frequency, the reptation mechanism gives way to fast intrachain motions (Rouse mechanism)[68] related to chain stretching on scales shorter than the contour length of the chains between entanglements l_e (see Fig. 10). In the experiment, the change of the relaxation mechanism in the high-frequency region is manifested by a simultaneous increase in the modules $G''(\omega)$ and $G'(\omega)$, whereas the Maxwell model predicts that $G'(\omega)$ would tend to a constant value, while $G''(\omega)$ would decrease (see Fig. 12).

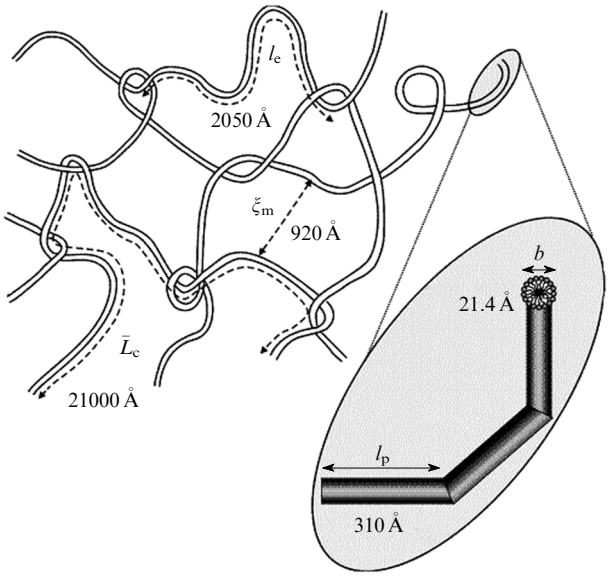


Figure 10. Characteristic scales of length in the spatial network of entangled wormlike (non-branched) aggregates.[73]
$\bar{L}_c$ is the average contour length; l_e is the contour length between the neighbouring entanglements; ξ_m is the length of the network cell; l_p is the persistence length of the chain; (b) the radius of the aggregate cross-section. The given values were measured for a solution of wormlike mixed micelles of cetyltrimethylammonium tosylate (CTAT) and sodium dodecyl benzene sulfonate (SDBS) with addition of hydrotropic salt (sodium tosylate) and excess of screening electrolyte (NaCl). The total surfactant concentration in the solution was 1.5% with the CTAT : SDBS ratio of 97 : 3 and 0.10% of sodium tosylate.

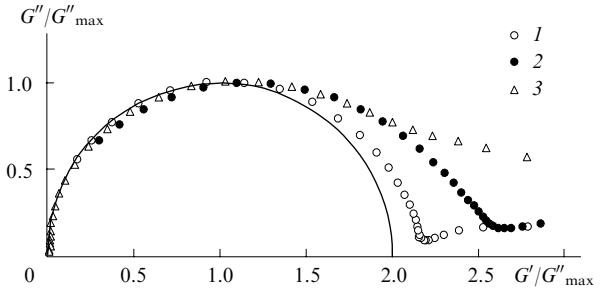


Figure 11. Cole–Cole diagram for a mixture of cetyltrimethylammonium 3-hydroxynaphthalene-2-carboxylate (CTAHNC) and cetyltrimethylammonium tosylate.[75]
G''_{max} is the maximum loss modulus at a frequency corresponding to the upper point of the semicircle. The dots are experimental data; the curve corresponds to the Maxwell model calculations. The total surfactant concentration is 100 mmol litre^{-1}; CTAHNC mole fraction: (*1*) 0, (*2*) 0.5, (*3*) 0.6; T = 303 K.

The change of the relaxation mechanism upon a frequency change gives rise to a minimum in the Cole–Cole plot (see Fig. 11); from the depth of this minimum, the numbers of entanglements per chain of the spatial network are estimated as [71, 74]

$$\frac{G''_{min}}{G'_\infty} \cong \frac{l_e}{\bar{L}_c} \tag{12}$$

where G''_{min} is the $G''(\omega)$ value in the minimum point, G'_∞ is the estimated value of the shear modulus (found in some studies by extrapolating the linear part of the Cole–Cole plot until it intersects the abscissa axis).[72] The frequency ω_{min} corresponding to the minimum is equal to $\sim 1/\tau_e$, where τ_e is the characteristic relaxation time of a chain with length l_e. Relation (12) holds provided that the characteristic time of chain breakage is substantially shorter than the reptation time but much longer than the relaxation time of chain segments between the entanglements:

$$\tau_{rep} \gg \tau_{break} \gg \tau_e$$

Presumably, the contour length of the chain segment between the neighbouring entanglements is considerably longer than the persistence length, which characterizes the chain flexibility (see Fig. 10).

If the above relations between the characteristic times start to be violated, the minimum in the Cole–Cole diagram becomes less deep. This increases the error of determination

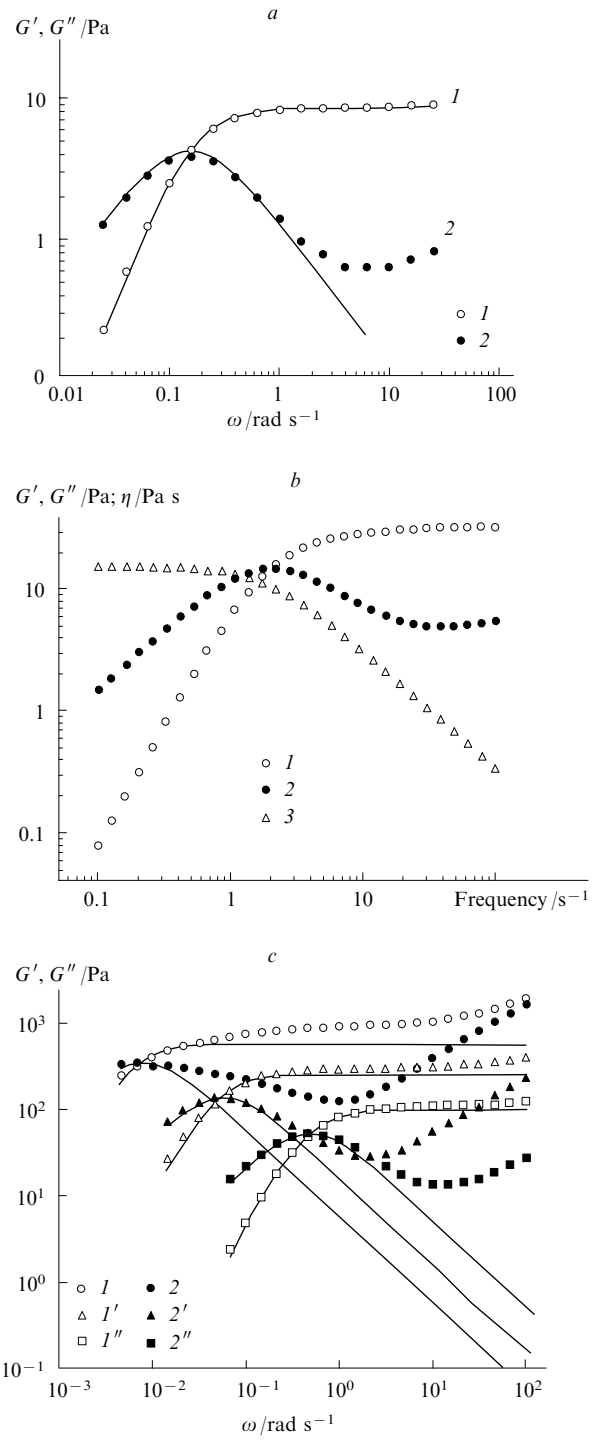


Figure 12. Frequency dependences of the storage modulus (*1*) and the loss modulus (*2*).
The dots are experimental data; the curves show approximation according to the Maxwell model.
(*a*) Aqueous solution of 50 mmol litre^{-1} of sodium oleate (NaOL) in the presence of 600 mmol litre^{-1} of KCl at 298 K;[76] (*b*) aqueous solution of NaOL mixed micelles at 298 K; the total surfactant volume fraction is 0.034; the mole fraction of NaOL is 0.23. The real part of the complex viscosity is shown (*3*);[72] (*c*) lecithin + citric acid solution in n-decane at 298 K.[77] Concentration (mass %): lecithin, 10; citric acid, 2.25 (*1*, *2*), 1.75 (*1′*, *2′*), 1.25 (*1″*, *2″*).[77]

of G'_∞ by extrapolating the linear segment of the plot. In this case, the shear modulus can be estimated as[72]

$$G'_\infty = 2G'(\omega_r) \cong 2G''_{max}$$

where the frequency ω_r is determined from condition (11).

The estimation of the number of entanglements per chain of the spatial network from Eqn (12) is suitable for determining the average contour length of the chains if l_e is known. For polymer networks, the latter value has been correlated with the persistence length of the chain and the spatial network cell dimension[43]

$$l_e = \frac{\xi_m^{5/3}}{l_p^{2/3}}$$

Using G'_∞ as the estimate for G_0, one has

$$G'_\infty = \frac{k_B T}{\xi_m^3} = \frac{k_B T}{l_e^{9/5} l_p^{6/5}} \tag{13}$$

Thus, Eqns (13) and (12) can be used to estimate the most important characteristics of the spatial network structure — l_e and $\bar{L}_c$ — from measured G'_∞ and G'_{min} if the persistence length of the chain l_p is known.

These relations make it possible to derive the concentration dependences of the viscosity and relaxation time basing on the theory developed for polymer chains. The reptation time of a flexible polymer in a semidilute solution is given by[68]

$$\tau_{rep} \sim \bar{L}_c^{\,3} \varphi^{3/2}$$

The characteristic time of breakage of the micellar chain τ_{break} is assumed to be inversely proportional to the mean chain length $\bar{L}_c$. In view of this, the equation for the relaxation time in the case of frequent chain breakage is

$$\tau_r = (\tau_{rep}\, \tau_{break})^{1/2} \sim \bar{L}_c \varphi^{3/4}$$

while in the case of rare breakage, one gets

$$\tau_r \approx \tau_{rep} \sim \bar{L}_c^{\,3} \varphi^{3/2}$$

The mean-field theory gives

$$G_0 = k_B T \varphi^{9/4}$$

irrespective of the average contour length of the chain. Thus, in the case of frequently breaking chains, the viscosity calculated from relation (10) is given by

$$\eta_0 \sim \bar{L}_c \varphi^3 \tag{14}$$

while in the case of rarely breaking chains, it is given by

$$\eta_0 \sim \bar{L}_c^{\,3} \varphi^{15/4} \tag{15}$$

In order to elucidate the concentration dependences of the viscosity and the relaxation time from the above relations, it is necessary to determine the dependence of the average chain length on the concentration. Below we consider different growth regimes of wormlike aggregates and how they influence the viscosity of the system.

III.2. Average chain length and viscosity of a non-ionic network

The contour length of wormlike micelles $\bar{L}_c$ varies over broad limits — from nano- to micrometres. Experimentally, this value can be estimated from the cryo-TEM images of the micelles. Useful information on the micelle growth and rigidity can be gained from LS and SANS data.[17] The free energy model of a solution of non-ionic linear chains subject to breakage and recombination, expressed in the mean force field approximation can be used to describe the equilibrium size distribution of chains.[70, 78] The average contour length of the chains

$$\bar{L}_c \sim 2\,\varphi^{1/2} \exp\frac{E}{2}$$

where E is the energy needed to break the chain. The polydispersity of chain length distribution is fairly high: the density of the number of chains of length L_c is proportional to the quantity $\exp(-L_c/\bar{L}_c)$.

Thus, in the fast breaking – recombination regime ($\tau_{break} \ll \tau_{rep}$), taking into account Eqn (14), the viscosity and relaxation time of the micelle network are expressed as

$$\eta_0 \sim \varphi^{7/2} \text{ and } \tau_r \sim \varphi^{5/4} \qquad (16)$$

In the slow breaking – recombination mode, the system behaves as a network of polydisperse polymer chains; the exponents are predicted by the classical reptation theory. Since $\bar{L}_c \sim \varphi^{1/2}$, one gets

$$\eta_0 \sim \varphi^{5.25} \text{ and } \tau_r \sim \varphi^3$$

The mean-field approximation used to estimate the power law exponents can be replaced by relations of the scaling theory for polymer systems.[43] In this case, the exponents of the concentration dependences ($\sim\varphi^{\alpha}$) would vary in the following way:[70, 79] $\alpha = -0.77$ for the linear dimension of the network cell; $\alpha = 2.31$ for the shear modulus, $\alpha = 0.6$ for the average length; $\alpha = 3.42$ for the chain reptation time in the slow breakage mode. In the fast breaking regime

$$\tau_r \sim \varphi^{1.41} \text{ and } \eta_0 \sim \varphi^{3.72}$$

The found concentration dependences of the viscosity and relaxation times are in good agreement with the experimental data for non-ionic surfactant micelles as well as for ionic surfactants at high salt concentration where the electrostatic interactions are considerably screened [in particular, for the CTAB + KBr and cetylpyridinium chloride (CPyCl) + sodium salycilate (NaSal) + NaCl systems].[80]

III.3. Growth of ionic micelles

Ionic micelles behave differently from non-ionic micelles. The breakage of ionic micelles can be facilitated by the electrostatic repulsion of the charged heads of the surfactant molecules. An important factor affecting the micelle growth is the entropy of counter-ions, which tend to condense near the cylindrical body rather than near the spherical ends of the micelle.

There are three distinct regimes of the growth of micelles.[78] In dilute solutions, the effective radius of electrostatic interactions far exceeds the average length of the micelle, and the average micelle length increases slowly (logarithmically) with the surfactant concentration. In this regime, the micelles are almost monodisperse.

A different growth regime is observed for semidilute solutions in which the radius of electrostatic interactions is smaller than the average micelle length. An increase in the surfactant concentration induces a fairly intense micelle growth. The average aggregate length is described by the relation [78]

$$\bar{L}_c \sim \varphi^{1/2} \exp\left[\frac{1}{2}\left(E - \frac{l_B b v^2}{\varphi^{1/2}}\right)\right] \qquad (17)$$

Here E is the breaking energy of neutral micelle; l_B is the Bjerrum length, b is the radius of the cylindrical part of the micelle, v is the effective charge per micelle unit length. The effective breaking energy decreases due to repulsion of the charged heads of surfactant molecules, which is reflected as a negative term of Eqn (17). The polydispersity of wormlike micelles is high (like that of non-ionic aggregates) but they grow faster with increase in the surfactant concentration and the growth cannot be described by a power law.[81]

The third growth regime is observed at high surfactant concentrations. The predominant ionic effect is then the entropy of mobile ions near the aggregate spherical ends. The micelle growth is described by nearly a power law [78]

$$\bar{L}_c \sim \varphi^{(1+\Delta)/2}$$

with the exponent greater than that for non-ionic micelles by $\Delta/2$, which is the value related to the net charge of the spherical ends and weakly (logarithmically) depending on φ. At higher ionic strengths (high salt or ionic surfactant concentration), the electrostatic contributions to the aggregate breaking energy are no longer significant due to screening of interactions, and the size distribution of micelles becomes, in essence, the same as for non-ionic micelles.

Thus, unlike non-ionic micelles, which grow according to a power law in both dilute and semidilute solutions, ionic micelles demonstrate a sharp transition from a weak growth (dilute regime) to a fairly intense growth (semidilute regime). Transitions from the slow growth to fast growth regime in a dilute solution were confirmed experimentally for many ionic surfactants.[82] This behaviour is controlled by electrostatic effects; when the charges are screened, the system behaves similarly to a system of non-ionic aggregates; therefore the high-concentration regime can be described by relations (16).

III.4. Flexibility of charged wormlike aggregates

The viscoelastic characteristics of the system depend on the flexibility of single chains. The chain flexibility is quantitatively characterized by persistence length (see Fig. 10), which is a measure of damping of orienational correlations along the chain. The persistence length of a wormlike aggregate is a key structural parameter, which is investigated in quite a number of experimental and theoretical works.[17] An important characteristic of the flexibility of ionic micelles is the electrostatic contribution to the micelle persistence length (l_p^{el}). Most researchers calculate l_p^{el} by the classical Odijk – Skolnick – Fixman (OSF) formula [83, 84] derived for polyelectrolyte chains based on the linear Poisson – Boltzmann equation in the limit of the vanishingly small thickness of the chain (charged thread). However, the

diameters of wormlike micelles far exceed the effective diameters of the chains of most linear polymers.[85]

The classical OSF theory was extended to charged wormlike particles of finite thickness.[86] Within the framework of a new theory based on the asymptotic expansions for the LPB equation in the toroid geometry, the electrostatic persistence length is given by the simple formula[86]

$$l_p^{el} = l_B v^2 b \kappa_D \left(1 + \frac{\kappa_D}{4b}\right) \quad (18)$$

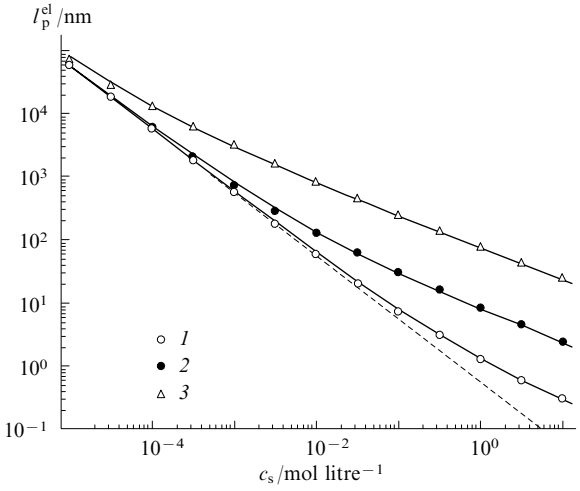


Figure 13. Electrostatic persistence length of a wormlike particle depending on the concentration of 1 : 1 electrolyte added (c_s).[86]
The dots show the numerical solution of the LPB equation; continuous lines correspond to calculations by Eqn (18): $b = 0.1$ (*1*), 1 (*2*), 10 nm (*3*); dashed line corresponds to OSF theory calculations; the linear charge density of micelles is 5.86 nm^{-1}.

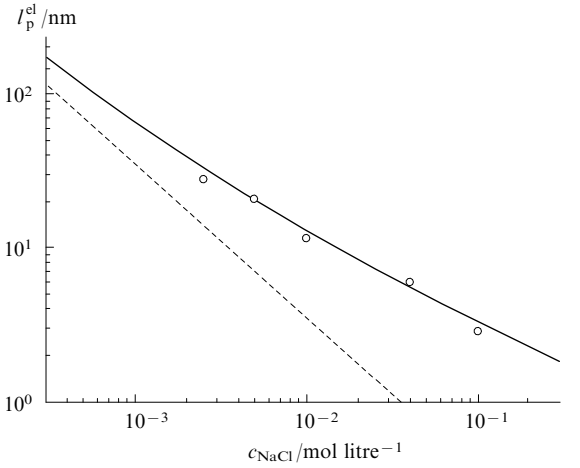


Figure 14. Electrostatic persistence length of a wormlike mixed micelle: hexaethylene glycol n-hexadecyl ether + sodium 1-hexadecanesulfonate in an aqueous solution of NaCl for different NaCl concentrations.
The $C_{16}E_6$ to $C_{16}SO_3$ Na weight ratio is 0.06. The dots are SANS data.[87] The continuous curve corresponds to calculations by Eqn (18), where $v = 1.46$ nm^{-1} and $b = 2$ nm; the dashed line corresponds to calculations according to the OSF theory.

here v is the linear charge density (in the elementary charge units) of wormlike micelles, b is the micelle radius, κ_D is the Debye radius. For a thread-like particle $b \to 0$, and formula (18) is degenerated into the classical expression of the OSF theory; for 'thick' micelles ($\kappa_D/4b \ll 1$) at high salt concentration, the persistence length varies linearly with the Debye radius:

$$l_p^{el} \sim \kappa_D$$

The agreement of the results obtained by formula (18) with the numerical solution of the LPB equation for wormlike particles of various thickness is shown in Fig. 13. It can be seen that the considered salt concentration range is fairly broad. The results of prediction by Eqn (18) and experimental data are presented in Fig. 14. It is noteworthy that the agreement with the experiment is much better than in the case of calculation by the classical OSF formula.

III.5. Viscosity and branching

The formation of micelle junctions considerably affects the dynamic characteristics of the system. As can be seen from Fig. 15, an addition of a salt to a solution of the ionic surfactant first causes viscosity to increase due to the linear growth and entanglement of wormlike micelles and then to decrease as micelle junctions appear and their concentration increases. The increase in the network fluidity is due to the mobility of junctions: they can easily slide along the micelle body, thus accelerating the stress relaxation.

The Cates kinetic model[70] was extended to systems of flexible branching micelles.[88, 89] The monoexponential pattern of system relaxation (and the ratio $G''_{min}/G'_{\infty} \cong l_e/\bar{L}_c$) are retained if the average effective chain length is defined as

$$\bar{L}_c \equiv \frac{l_p \rho}{\rho_e + 2\rho_j} \quad (19)$$

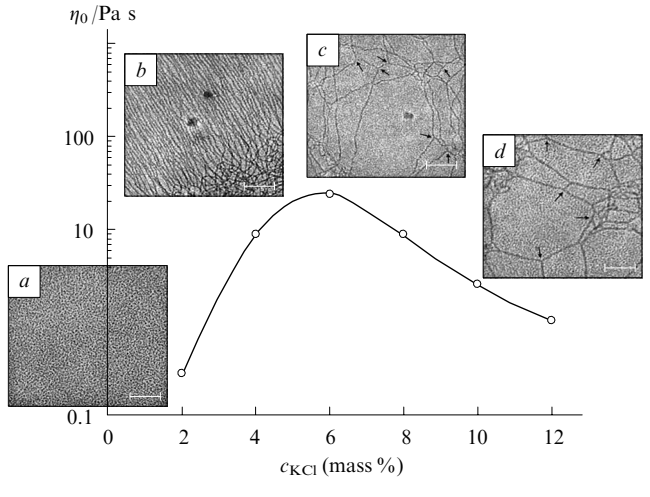


Figure 15. Viscosity at a zero shear rate *vs.* salt (KCl) concentration for a solution containing 1.5 mass % of erucyl bis(hydroxyethyl)methylammonium chloride (EHAC) at 313 K.[17]
(*a*–*d*) Cryo-TEM images corresponding to 0 mass %, 2 mass %, 6 mass % and 12 mass % KCl show the transformation of spherical micelles to wormlike micelles and, after the viscosity maximum has been passed, the formation of a network of branched aggregates. The scale shown in the micrographs is 100 nm.

where ρ_e is the concentration of ends, ρ_j is the concentration of trifuncional junctions, ρ is the concentration of the linear chain segments that form the wormlike aggregate body (this concentration is proportional to the surfactant volume fraction).

If the energy of chain breakage does not depend on the composition of the solution (which is the case for non-ionic or highly screened ionic aggregates), the chain breaking–recombination equilibrium means [49,89] that

$$\rho_e \sim \varphi^{1/2} \text{ and } \rho_j \sim \varphi^{3/2}$$

Thus, for a system containing only linear (non-branched) micelles

$$\bar{L}_c \sim \varphi^{1/2}$$

In the other limit, that is, for a junction-saturated network (the contour length between the junctions is equal to the correlation radius), $\rho_e = 0$, while $\bar{L}_c$ is equal to the average chain length between the junctions. Then in the absence of electrostatic interactions

$$\bar{L}_c \sim \varphi^{-1/2}$$

Thus, for a junction-saturated non-ionic network in the fast chain breaking regime, the characteristic time of stress relaxation is

$$\tau_r \sim \varphi^{1/4}$$

and the viscosity is

$$\eta_0 \sim \varphi^{5/2} \qquad (20)$$

The change in the exponent is caused by an increase in the fraction of junctions and is not related to shortening of linear chains.

In reality, some intermediate behaviour of the system is most likely, as both junctions and ends make their contributions. Thus, the power law exponent for the quantity

$$\frac{G''_{min}}{G'_{\infty}} \sim \frac{l_e}{\bar{L}_c}$$

will be lower than the calculated value of $-7/4$, which is predicted by theory for a network of non-branched entangled micelles ($l_e \sim \xi_m^{5/3}$, $\xi \sim \varphi_m^{-3/4}$ for a good solvent). In the limit of a junction-saturated network, the calculated exponent is $-3/4$ (Ref. 89). A close value, namely -0.77, has been obtained [89] from experimental data for the CTAB + KBr system at high salt concentration. The experimental concentration dependences of τ_r and η_0 for this system are consistent with the assumption that a network with junctions is present. For a network of reverse lecithin micelles in an isooctane + water mixture,[90] the exponent of the concentration dependence of the average chain length between the junctions is -0.55 ± 0.07, *i.e.*, it is also quite close to the value predicted for the saturated network.

The presence of junctions accounts for the decrease in the relaxation time at high surfactant concentration in salt-free solutions of cetyltrimethylammonium hydroxynaphthalene carboxylate.[82] The addition of a salt to a dilute solution of the micelles of this surfactant also induces branching. In a salt solution, the increase in the viscosity with increase in the surfactant concentration is described by exponent of 2.3 close to that in Eqn (20) for a junction-saturated network.

The above examples of systems illustrate experimental evidence supporting the theory; however, limitations for the views being discussed are also known.[91,92] For aqueous mixtures of cationic and anionic surfactants, regimes corresponding to networks of branching micelles and networks of linear entangled micelles were experimentally identified.[72] The theory implies the same exponent for the concentration dependence of the shear modulus (2.25) in the branching and entangled network regimes; the experimental values obtained for these regimes are different. In the case of branching micelles, the theoretical predictions for the viscosity and shear modulus are in line with the experiment. For linear micelles, the theory gives underestimated exponent values. Analogous results were obtained in an experimental study of the viscosity and shear modulus for reverse micelles of mixtures of lecithin and multivalent carboxylic acids in decane.[77]

It is also known that the rheological behaviour of solutions of wormlike micelles of some surfactants resists description in terms of the monoexponential Maxwell model. Some systems are characterized by a spectrum of relaxation times,[20] some other form elastic gels [2] the response of which depends little on the deformation rate. As noted above, the views developed in this paper do not apply to rigid chain systems ($l_p \sim l_e$) or to the systems in which strong interchain interactions give rise to rigid ordered structures.[2] This review does not cover glass-like colloid [14,93–95] and polymeric [36] gels and the self-assembly in micellar or polymer solutions under the action of shear stress.[24,37,96–98] It is noteworthy that this field of nonlinear rheology is being actively developed [99,100] and, probably, some phenomena such as the appearance of differently oriented regions of strong and weak shear stresses,[101] deformation-induced liquid-crystalline ordering, phase separation, occasional appearance and vanishing of short-lived ordered structures, rheochaos and so on [23] are common to solutions containing extended wormlike particles [102] in which orientational correlations are possible.[38,39] Currently, the key patterns of the behaviour of such systems in various concentration regimes have been established.[37]

Apart from the micellar systems, the Cates model can be used to interpret the data of rheological measurements for polymer chain networks (of metal complexes,[10,103,104] polyelectrolytes [105] and other compounds [9,106]) in which the interchain cross-links are provided by weak physical interactions.[107] Breaks of the cross-links over time periods much shorter than the chain reptation time provide the major relaxation mechanism, and the system is described by the Maxwell model with only one relaxation time (Fig. 16). A similar behaviour is displayed by spatial networks consisting of microemulsion droplets connected by polymer chains hydrophobized at the ends.[3,4,11,108,109] When the interchain cross-links are strengthened, the system behaviour deviates from that described by the Cates model (Fig. 17),[9,12,110] which is manifested, in particular, as the difference between the exponents of the concentration dependences of the viscosity (2.8 instead of 3.5) [10] and the diffusion coefficient.[103] This behaviour is well described in terms of the reptation and sticking model of Rubinshtein and Semenov,[111] which extends the dynamic Cates reptation model to

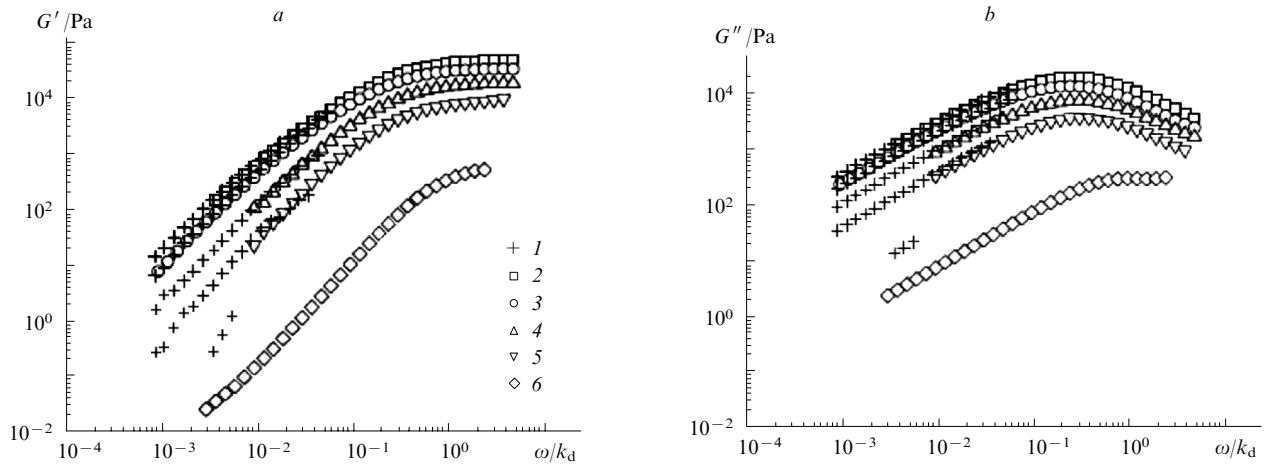


Figure 16. Frequency dependences of the storage modulus (*a*) and the loss modulus (*b*) for a solution of 0.11 g ml^{-1} of poly-4-vinylpyridine in dimethyl sulfoxide at various concentrations of bis-palladium(II) agents of different structure responsible for physical interchain cross-links.[10]
Rate constants for dissociation of cross-links k_d = 1450 (*1*) and 17 s^{-1} (*2*–*6*). The concentrations of the one (*1*) and the other (*2*–*6*) cross-linking agents are constant for the presented curves and increase on going from lower to upper curves: 1% (*1* , *6*), 2% (*1*, *5*), *3*% (*1*, *4*), 4% (*1*, *3*), 5% (*1*, *2*). T = 298 K.

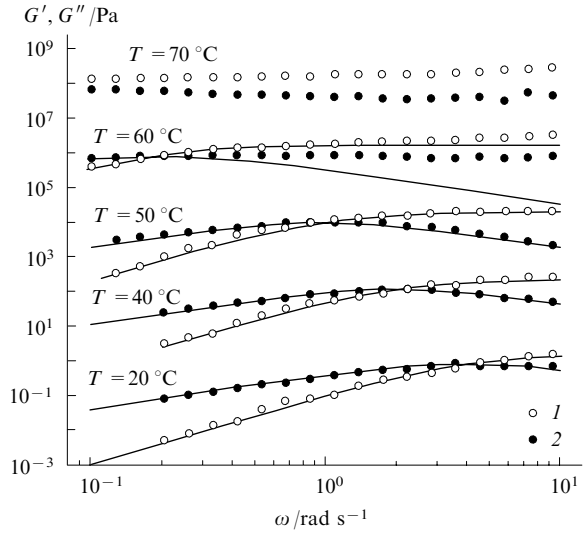


Figure 17. Frequency dependences of the storage modulus (*1*) and the loss modulus (*2*) for an aqueous solution containing 0.4 mass % of polyacrylamide hydrophobized by oxyethylene fragments at various temperatures.[9]
At 60 and 70 °C, the data noticeably deviate from the Maxwell model description (lines). Data for temperatures of 40–70 °C are shifted along the ordinate axis. The shifts are: 10^2 (40 °C), 10^4 (50 °C), 10^6 (60 °C), 10^8 (70 °C).

sticking chain systems. Currently, theoretical models of these systems are being developed.[112–114]

III.6. Effect of ion specificity on the micellar growth

The nature of ions in solution considerably affects the micellar growth and the pattern of the concentration dependence of the viscosity.[75, 115] The counter-ions containing hydrophobic groups, in particular, salicylates or benzoates, can strongly bind to the aggregate.[116] By penetrating into a micelle and decreasing the spontaneous curvature, these ions stimulate the growth and branching of aggregates. This, as has been discussed above, results in the appearance of a viscosity maximum with increase in the salinity. The addition of a NaSal salt to solutions of CTAB and CPyCl gives rise to a second viscosity maximum at high salt concentration.[117, 118] The presence of two maxima is attributable to non-monotonic variation of the density of junctions in a micellar network. Note that for some systems, reduction of the micellar size was detected in the presence of a high concentration of salts containing penetrating ions.[119] In this case, the observed viscosity maximum is due to the opposite trend: an increase in the spontaneous curvature and the presence of a maximum in the plot for the average aggregation number *vs*. the concentration of the salt added.

Systematic studies using various salts (unable to penetrate into the micelle) added to a solution of CTAB [118] demonstrated that the binding of counter-ions to the micelle surface leads to a decrease in the persistence length and more intense growth of viscosity with increase in the salt concentration.

The observed effects of the nature of ions are often fairly subtle. Indeed, the replacement of KCl added to a solution of EHAC by NaCl has a pronounced influence on the position of the viscosity peak: the salt concentration at which the viscosity is maximum is several-fold higher for K^+ co-ions than for Na^+ co-ions. However, the expected weak effect of most co-ions on the critical micelle concentration (CMC) and the salt-induced sphere–rod transition threshold solutions of ionic surfactants was confirmed experimentally.[120]

The account for the effect of ion specific character on the growth of aggregates and the viscoelastic behaviour of the solution is a still unsolved problem. Nevertheless, certain achievements along this line can be noted.

The experimentally established effect of the nature of counter-ions on the formation and growth of ionic surfactant micelles can be qualitatively interpreted [120] within the framework of the Collins phenomenological concept:[121]

chaotropic counter-ions form more compact ion pairs with the chaotropoic heads of the surfactant molecules, while for cosmotropic ions, these are cosmotropic heads. The compactness of the ion pair between the mobile ion and the charged head of the surfactant molecule in the micelle corona affects the spontaneous curvature of the aggregate, *i.e.*, this controls the tendencies to growth and branching. This concept has been expressed quantitatively in the molecular thermodynamic models, which adequately describe micelle formation [34, 122, 123] and micellar growth [34, 35] in solutions of classical cationic and anionic surfactants in the presence of ordinary salts. According to these models, the key factors that control the specific ion effects during aggregation are the proper size, dispersion interactions with the micelle and different degrees of hydration of mobile ions having penetrated into the micelle corona. In conformity with the Collins concept, the hydration effects in the corona are determined by the combination of a mobile ion and a surfactant molecule head. The subtle balance of the contributions taken into account by the models makes it possible to describe the quantitative and qualitative differences in the effect of salt nature on the surfactant aggregation. Indeed, the addition of some salts can induce only the growth of aggregates, while for the other salts, the model predicts the initial growth of micelles, which is replaced by micelle size reduction at high salt concentrations. An explanation to the pronounced effect of the co-ion nature on the position of the viscosity peak and rather weak co-ion sensitivity of the CMC and salt-induced sphere – rod transition thresholds was reported for the first time.[35]

IV. Materials and devices based on micellar systems

The reversibility of the micelle growth and disintegration processes provides the possibility to control the substance solubilization, while the reversibility of the formation and destruction of the spatial networks of wormlike micelles can serve to control the viscoelastic properties of solutions. This makes solutions of wormlike micelles highly attractive for solving a variety of practical problems in petrochemistry, pharmacology and biomedicine.

The tendencies of micelle aggregates to grow and branch depend on the preferred packing of molecules into aggregates of various shapes and spontaneous curvatures, which is determined by the chemical individuality, that is, the molecular portrait of the system and changes upon a change in the conditions. The molecular portrait determines the system sensitivity to various factors: the growth and the formation of wormlike micelle networks can be controlled by changing the surfactant concentration, temperature,[124] pH [125] and electric field,[2] by irradiation of the solution,[126] by introduction of various additives and varying their concentrations. Adjustment of single surfactants and additives or their combinations opens up a rather easy and effective way for the search for new materials with a controlled response. The currently known systems of smart wormlike micelles sensitive to the change of various factors were considered in detail in a recent review.[2] Below, examples of systems important for practical applications are given and basic scheme of their applications are discussed.

Viscoelastic solutions of surfactants are used for hydraulic fracturing of formations for enhanced oil recovery.[18] The hydraulic fracturing gives rise to numerous fractures in the rock, which allow oil to flow into the boreholes to withdrawal points and thus the oil recovery is enhanced. To prevent these newly formed fractures from collapsing, which would arrest the oil flow, they are filled with various finely grained materials (sand, glass beads, walnut shell fragments, *etc.*). A viscous liquid is required to deliver the filler into fractures. After the delivery has been completed, the liquid should become easy-flowing and leave the filler in the rock fractures without interfering with the oil flow. The desired behaviour may be inherent in solutions of wormlike micelles: the spatial micelle network accounts for high viscosity; however, upon contact with hydrocarbons in oil-bearing formation pores and fractures, wormlike aggregates either turn into spherical aggregates or form a microemulsion.[127] This transformation is accompanied by a decrease in the solution viscosity and, hence, the solution is removed without plugging the pores, while the filler remains in the formation. Widely used carrier liquids are solutions of cationic quaternary ammonium salts containing 18 to 22 carbon atoms in the hydrocarbon tail of the molecule (these salts are obtained from the rapeseed oil). The application of these systems is limited to moderate temperatures; by using EHAC with addition of sodium salicylate to enhance the micellar growth, it is possible to raise the temperature limit to 366 K.[2]

A notable feature of wormlike particles, namely, the ability to reduce the resistance to liquid flow in a pipe, is used for oil transport, for heating and air conditioning system pipelines, for irrigation, waste water discharge and fire extinguishing systems and so on.[2, 18] A benefit of wormlike micelles compared with linear polymers used for the same purpose is that micelles that have broken due to high stress are able to recombine and maintain the system efficiency. By reducing the resistance to flow in domestic heating systems, a substantial energy saving was achieved in some regions of Denmark, the USA, Japan and Canada.[17] However, surfactant solutions that reduce the resistance to flow also reduce the heat flux. The viscous boundary formed near the pipe wall and decreasing the resistance to flow retards the heat transfer to the wall, which is undesirable in heating systems. An idea for solving this problem has been put forward: it has been proposed to use photosensitive systems of wormlike micelles the growth of which is controlled by external irradiation.[6] Cationic surfactants (CTAB or erucyl dimethylamidopropyl betaine) with the organic counter-ion of *trans*-*o*-methoxycinnamic acid (*trans*-OMCA), which forms long wormlike micelles, are used. As the solution before the heat exchanger inlet is exposed to UV radiation, the counter-ion is converted to the *cis*-form (*cis*-OMCA) and packing into shorter aggregates becomes preferred. Thus, owing to light sensitivity of the surfactant counter-ion, the system viscosity can be changed. The viscosity of the solution in the heat exchanger decreases by several orders of magnitude and the heat exchange becomes effective. However, attempted preparation of photoreversible systems based on commercially available OMCA failed.[2] The photoreversibility of rheological response was found for an aqueous solution of a mixture of a cationic surfactant, oleyl bis(2-hydroxyethyl)methyl ammonium chloride (3.4 mmol litre^{-1}) and sodium 4-phenylazobenzoate (ACA, 2 mmol litre^{-1}).[128] The alternating

exposure of the solution to UV and visible light induces the transition of ACA from the *trans*- to *cis*-configuration and back. This results in the destruction and restoration of wormlike micelles, which can be used to control the heat exchange and resistance to flow.

An interesting example of the photoreversibility of the rheological response is a solution of CTAB and salicylic acid in which a network of entangled micelles is formed upon the addition of a small amount (1%) of photoactive 2,4,4′-trihydroxychalcone (Ct).[129] UV irradiation induces *trans*–*cis* isomerization of Ct, rearrangement of wormlike micelles and a viscosity change. This is accompanied by a change in the solution colour, which enables visual monitoring. Without irradiation, the sample is yellowish and has a viscosity of 7 Pa s (for a shear rate of 0.5 s^{-1}). On exposure to solar light, the sample colour changes to dark orange in several minutes due to the transformation of Ct into the flavylium cation. As this takes place, the viscosity of the solution decreases by a factor of 2. As the irradiation is terminated, the initial state of the solution is restored; however, this requires $\sim$ 40 min. Currently, studies of the systems of light-controlled wormlike micelles are in progress.[2, 17, 128]

Attention is drawn by micellar solutions in which the viscosity is controlled by external electric field. These systems can be used in hydraulic seals, valves, transmissions, ink-jet printers and so on. A micellar solution of this type was prepared using alkyltrimethylammonium surfactant chemically modified by introduction of a ferrocenyl group at the end of the hydrocarbon tail of the molecule. The surfactant thus formed — 11-ferrocenylundecyltrimethylammonium bromide — forms wormlike micelles in the presence of sodium salicylate.[130] The ferrocenyl group is hydrophobic and its oxidized form (ferricinyl cation) is hydrophilic. The conversion of this group from the oxidized to the reduced form upon the application of an electric field induces a change in the lipophilic–hydrophilic balance and transformation of the network of wormlike micelles into separate globular aggregates. Thus, by controlling the redox reaction, it is possible to control the micellar growth.

Temperature variation is also a way to control the micellar growth and viscoelastic properties (see above). Most of the studied solutions of wormlike surfactant micelles form 'soft' gels the viscoelastic behaviour of which is described by the Maxwell model. However, in some systems, 'hard' (elastic) gels are formed upon temperature change, the mechanical characteristics of the system change by several orders of magnitude and depend little on frequency.[2] Heating of a 1.0 M solution of 3-(*N*-palmitamidopropyl-*N*,*N*-dimethylammonium)propanesulfonate in the presence of 0.5 M NaCl from 303 to 313 K induces reversible transformation of a viscous micellar solution into an elastic spatial network.[131] Solutions of wormlike micelles of an ionic liquid, 1-hexadecyl-3-methylimidazolium bromide, with NaSal (Ref. 132) and erucyl dimethylamidopropyl betaine[133] form elastic gels at temperatures below 293 and 313 K, respectively.

Micellar gels hold much promise as a possible alternative to polymer hydrogels widely used in biomedical applications: for tissue transplantation and repair, drug delivery, development of sensor devices and so on.[2, 17] Of interest are the properties of a polymer gel, which is soft and ductile at room temperature and elastic at the body temperature; therefore, polymeric inner soles for shoes acquire and preserve the unique shape of a particular human foot.[134] Polymer gels are used in the development of sensor devices with response to glucose for the controlled insulin administration into diabetes mellitus patients.[135] Other smart materials based on polymer gels were also devised.

A smart micellear gel can also be designed to be sensitive to the presence of a particular chemical compound in a solution and used in sensing devices. The transformation of a micellar solution into a hydrogel at a human body temperature opens up a theoretical possibility to avoid surgery in the tissue implantation. The value of micelles for controlled drug delivery is related to their ability to solubilize hydrophobic molecules of pharmaceutical drugs and release the drugs in response to a change in the external conditions.

Solutions of wormlike micelles of biocompatible surfactants, in particular, lecithin,[20, 136] receive increasing attention of researchers. Biocompatible lecithin is widely used in food industry and in the manufacture of cosmetic formulations. Lecithin-based wormlike micelles are used as model systems in the development of methods for transdermal delivery of biologically active substances such as caffeine and theophylline.[136] A related chemically modified surfactant, dilauryl phosphatidyl nucleoside, combines the aggregative properties of lecithin and functions of molecular recognition of heterocyclic bases in nucleic acids.[137] Phospholipid-based surfactants that form wormlike micelles are promising for pharmacological applications and selective delivery of DNA genetic material to the cells.[2] Generally, the considered systems have been less studied than solutions of classical surfactants and now these studies have been intensified.

Combinations of wormlike surfactant micelles with polymers, nanoparticles and biomaterials open up extensive opportunities for the design of hybrid functional materials.[2, 17]

This application area is new; nevertheless, the obtained results attest to good prospects of smart wormlike micelles. Of primary importance is to establish the relationship between the macroscopic behaviour, morphology and molecular characteristics of such systems and to advance the methods of the molecular thermodynamic prediction.

V. Conclusion

In this review, we traced the universal patterns of behaviour of the systems capable of reversible formation of spatial networks: the general features manifested in the structure and macroscopic properties of the system irrespective of the molecular structure of the chains. This universal character is interpreted in terms of the concept of entropic spatial network the structure and equilibrium properties of which are controlled by thermal defects — junctions and chain ends. Networks of this type are formed in bicontinuous microemulsions, fluids of dipole solid spheres, in many physical polymer gels, solutions of Janus micelles and wormlike micelles of surfactants. The free energies of thermal defects are determined by the chemical individuality, *i.e.*, the molecular 'portrait' of the system, which is manifested quite obviously. Indeed, although the gel formation and phase separation are controlled by the balance of thermal defects, they are observed on cooling for some systems and on heating for other systems. This refers, for example, to micellar systems. The molecular architecture

dictates the preferred packing into aggregates of one or another shape and, hence, the balance of junctions and ends for wormlike micelles in the solution. The chemical effects of components (surfactant isomerization and functionalization and the natures of the solvent and the added salt) are often subtle, which complicates the quantitative description for them.

The universal behaviour is also inherent in the dynamic properties of the system of growing and breaking chains. A relationship can be traced between the aggregate tendency to grow and branch, the solution structure and the results of rheological measurements. It is noteworthy that the viscoelastic behaviour of a polydisperse system of chains experiencing frequent breakage is reflected (in the case of moderate shear frequencies) by the simple Maxwell model. This rheological behaviour is observed for the vast majority of solutions of wormlike micelles studied to date (although there are exceptions). The chemical nature of the system shows itself in the different characteristic relaxation times, different aggregate growth regimes, various types of response to a change in the conditions (concentration, temperature, the nature of additives present in the system, exposure to UV radiation and so on).

The accumulation of empirical knowledge about the behaviour of solutions of wormlike micelles is still somewhat ahead of the development of the quantitative molecular thermodynamic theory. However, certain progress has been made along the latter line. The research group to which the authors of this review belong has developed molecular thermodynamic models for branching wormlike micelles and networks formed by classical ionic surfactants,[31, 61] ionic diblock copolymers,[138, 139] including pH-sensitive ones;[32] and uncommon pH and salinity effects in the change of morphology and mechanical behaviour of aggregates were described.[33] Molecular thermodynamic models of pH-sensitive mesostructural diblock copolymer gels [140] and gels formed in cross-linked polymer solutions [30] were developed. The classical OSF theory for the electrostatic component of the chain rigidity was extended to charged micellar aggregates considering their finite thickness.[86] A molecular thermodynamic approach suitable for describing the effect of the nature of an 1 : 1 inorganic salt on the formation and growth of wormlike micelles in solutions of classical ionic surfactants was developed.[34] The effects of counter-ions and co-ions were considered within a unified approach and a mechanism explaining for the first time the significant role of the co-ion at high salt concentration was proposed.[35]

It appears that further development of the methods of molecular thermodynamic modelling would be related first of all to more detailed description of the micellar aggregate structure and more detailed consideration of specific and non-specific intermolecular interactions of its components. These methods can be useful for the targeted search for micellar systems with specified properties. For instance, the recently proposed model for mixed non-ionic surfactant micelles [141] reflects the complex structure of the micelle corona, the presence of specific interactions between various functional groups of components and hydration. The model was formulated in a group variant using interaction parameters of functional groups estimated previously from the data on the phase equilibria for a broad range of mixtures.[142, 143] The development of models of this type is important, in particular, for predicting the distribution of organic molecules between micelles and the surrounding solution.[144 – 146]

The possibility to control the growth of aggregates and the viscoelastic properties of the system enables addressing other practical problems. For example, for solutions of wormlike surfactant micelles, by selecting the appropriate molecular 'portrait', it is possible to obtain systems with viscosity and elastic modulus being able to reversibly change by several orders of magnitude upon the change in the pH or temperature or upon application of electric field and so on. Currently, such smart systems of wormlike micelles are already used in petroleum production and in indoor heating installations. The extensive prospects for the practical use of these systems are related to the design of new sensors, artificial tissues and controlled drug delivery.

This review was written with the financial support of the Saint Petersburg State University (Project Nos 12.38.199.2014, 12.50.1559.2013) and the Russian Foundation for Basic Research (Project No. 13-03-00981-a).

Figure 1 reprinted with permission. Copyright by the American Physical Society; Figs 2, 7 and 15 reprinted with permission. Copyright by the Royal Chemical Society; Figs 3 – 6, 9 – 12 *a*,*b* and 16 reprinted with permission. Copyright by American Chemical Society; Figs 8 and 12 *c* reprinted with permission. Copyright by Elsevier; Fig. 13 reprinted with permission. Copyright by AIP Publishing LLC; and Fig. 17 reprinted with permission. Copyright by Wiley.

References

1. X-J Wu, Y Wang, W Yang, B-H Xie, W Yang, W Dan *Soft Matter* **8** 10457 (2012)
2. Z Chu, S A Dreiss, Y Feng *Chem. Soc. Rev.* **42** 7174 (2013)
3. E Michel, J Appell, F Molino, J Kieffer, G Porte *J. Rheol.* **45** 1465 (2001)
4. M Filali, M J Ouazzani, E Michel, R Aznar, G Porte, J Appell *J. Phys. Chem. B* **105** 10528 (2001)
5. S Kantorovich, J J Cerda, C Holm *Phys. Chem. Chem. Phys.* **10** 1883 (2008)
6. M Klokkenburg, R P A Dullens, W K Kegel, B H Erne, A P Philipse *Phys. Rev. Lett.* **96** 037203 (2006)
7. M Klokkenburg, B H Erne, J D Meeldijk, A Wiedenmann, A V Petukhov, R P A Dullens, A P Philipse *Phys. Rev. Lett.* **97** 185702 (2006)
8. T Tlusty, S A Safran *Science* **290** 1328 (2000)
9. X Zhang, X Jiang, X Zhang, H Dai *J. Polym. Sci., Part B: Polym. Phys.* **48** 1799 (2010)
10. D Xu, S L Craig *Macromolecules* **44** 5465 (2011)
11. J Sprakel, E Spruijt, M A C Stuart, M A J Michels, J van der Gucht *Phys. Rev. E* **79** 056306 (2009)
12. F van de Manakker, T Vermonden, N el Morabit, C F van Nostrum, W E Hennink *Langmuir* **24** 12559 (2008)
13. D de las Heras, J M Tavares, M M Telo da Gama *Soft Matter* **7** 5615 (2011)
14. P J Lu, D A Weitz *Annu. Rev. Condens. Matter Phys.* **4** 1 (2013)
15. T Tlusty, S A Safran *J. Phys.: Condens. Matter* **12** A253 (2000)
16. P Brown, C P Butts, J Eastoe *Soft Matter* **9** 2365 (2013)
17. S A Dreiss *Soft Matter* **3** 956 (2007)
18. S Ezrahi, E Tuval, A Aserin *Adv. Colloid Interface Sci.* **128 – 130** 77 (2006)
19. Z Rao, M Inoue, M Matsuda, T Taguchi *Colloids Surf., B* **82** 196 (2011)
20. G Palazzo *Soft Matter* **9** 10668 (2013)

21. L M Walker *Curr. Opin. Colloid Interface Sci.* **14** 451 (2009)
22. M E Cates, S M Fielding *Adv. Phys.* **55** 799 (2006)
23. M Cates, S Fielding, in *Giant Micelles: Properties and Applications* (Eds R Zana, E W Kaler) (Boca Raton, FL: CRC Press, 2007) p. 109
24. S Lerouge, J F Berret, in *Polymer Characterization* (Eds K Dusek, J-F Joanny) (Berlin: Springer, 2010) p. 1
25. N A Smirnova *Russ. Chem. Rev.* **74** 129 (2005)
26. A I Rusanov *Mitselloobrazovanie v Rastvorakh Poverkhnostnoaktivnykh Veshchestv* (Micelle Formation in Solutions of Surfactants) (St Petersburg: Nauka, 1992)
27. R Nagarajan, E Ruckenstein, in *Equations of State for Fluids and Fluid Mixtures* (Eds J V Sengers, R F Kayser, C J Peters, H J White) (Amsterdam: Elsevier, 2000) p. 589
28. T Tlusty, S A Safran *Philos. Trans. R. Soc., London, Ser. A* **359** 879 (2001)
29. J Russo, J M Tavares, P I C Teixeira, M M Telo da Gama, F Sciortino *Phys. Rev. Lett.* **106** 085703 (2011)
30. S Tcyrulnikov, A I Victorov *Macromolecules* **46** 4706 (2013)
31. V A Andreev, A I Victorov *Langmuir* **22** 8298 (2006)
32. A I Victorov, N V Plotnikov, P-D Hong *J. Phys. Chem. B* **114** 8846 (2010)
33. A Victorov *Soft Matter* **8** 5513 (2012)
34. S V Koroleva, A I Victorov *Langmuir* **30** 3387 (2014)
35. S V Koroleva, A I Victorov *Phys. Chem. Chem. Phys.* **16** 17422 (2014)
36. A L Volynskii, A Y Yarysheva, E G Rukhlya, L M Yarysheva, N F Bakeev *Russ. Chem. Rev.* **83** 1003 (2014)
37. A Y Malkin, A V Semakov, V G Kulichikhin *Adv. Colloid Interface Sci.* **157** 75 (2010)
38. S Lerouge, M A Fardin, M Argentina, G Gregoire, O Cardoso *Soft Matter* **4** 1808 (2008)
39. J F Berret, in *Molecular Gels: Materials with Self-Assembled Fibrillar Networks* (Eds R G Weiss, P Terech) (Berlin: Springer, 2006) p. 667
40. S R Derkach *Reologiya Emul'sii* (Rheology of Emulsions) (St Petersburg: Nauka, 2012)
41. S R Raghavan, H Edlund, E W Kaler *Langmuir* **18** 1056 (2002)
42. A Bernheim-Groswasser, T Tlusty, S A Safran, Y Talmon *Langmuir* **15** 5448 (1999)
43. P G de Gennes *Scaling Concepts in Polymer P hysics* (Ithaca, New York: Cornell University Press, 1979)
44. T J Drye, M E Cates *J. Chem. Phys.* **96** 1367 (1992)
45. L F Vega, G Jackson *Fluid Phase Equilib.* **306** 1 (2011)
46. A N Semenov, M Rubinstein *Macromolecules* **31** 1373 (1998)
47. M Rubinstein, A N Semenov *Macromolecules* **31** 1386 (1998)
48. M Rubinstein, R H Colby *Polymer Physics* (Oxford: Oxford University Press, 2003)
49. K Elleuch, F Lequeux, P Pfeuty *J. Phys. I (France)* **5** 465 (1995)
50. G Cristobal, J Rouch, J Curely, P Panizza *Physica A: Stat. Theoret. Phys.* **268** 50 (1999)
51. A G Zilman, S A Safran *Phys. Rev. E* **66** 051107 (2002)
52. A Zilman, J Kieffer, F Molino, G Porte, S A Safran *Phys. Rev. Lett.* **91** 015901 (2003)
53. R Nagarajan, E Ruckenstein *Langmuir* **7** 2934 (1991)
54. A Goldsipe, D Blankschtein *Langmuir* **22** 3547 (2006)
55. S A Safran *Adv. Phys.* **48** 395 (1999)
56. A Zilman, S A Safran, T Sottmann, R Strey *Langmuir* **20** 2199 (2004)
57. T Tlusty, S A Safran, R Strey *Phys. Rev. Lett.* **84** 1244 (2000)
58. L K Shrestha, R G Shrestha, K Aramaki, G Yoshikawa, K Arida *J. Phys. Chem. Lett.* **4** 2585 (2013)
59. S Murgia, G Palazzo, M Mamusa, S Lampisa, M Monduzzi *Phys. Chem. Chem. Phys.* **13** 9238 (2011)
60. G Porte, R Gomati, O El Haitamy, J Appell, J Marignan *J. Phys. Chem.* **90** 5746 (1986)
61. V A Andreev, A I Victorov *Mol. Phys.* **105** 239 (2007)
62. S May, Y Bohbot, A Ben-Shaul *J. Phys. Chem. B* **101** 8648 (1997)
63. I Szleifer, M A Carignano, in *Advances in Chemical Physics: Polymeric Systems* Vol. 94 (Eds I Prigogine, S Rice) (New York: Wiley, 1996) p. 165
64. E B Zhulina, O V Borisov *Macromolecules* **38** 6726 (2005)
65. E B Zhulina, T M Birshtein, O V Borisov *Eur. Phys. J., E* **20** 243 (2006)
66. D Danino *Curr. Opin. Colloid Interface Sci.* **17** 316 (2012)
67. J Appell, G Porte, A Khatory, F Kern, S J Candau *J. Phys. II* **2** 1045 (1992)
68. M Doi, S F Edwards *The Theory of Polymer Dynamics* (Oxford: Clarendon Press, 1986)
69. M E Cates *Macromolecules* **20** 2289 (1987)
70. M E Cates, S J Candau *J. Phys.: Condens. Matter* **2** 6869 (1990)
71. R Granek, M E Cates *J. Chem. Phys.* **96** 4758 (1992)
72. P Koshy, V K Aswal, M Venkatesh, P A Hassan *J. Phys. Chem. B* **115** 10817 (2011)
73. B A Schubert, E W Kaler, N J Wagner *Langmuir* **19** 4079 (2003)
74. P A Hassan, S J Candau, F Kern, C Manohar *Langmuir* **14** 6025 (1998)
75. M S Turner, M E Cates *Langmuir* **7** 1590 (1991)
76. G C Kalur, S R Raghavan *J. Phys. Chem. B* **109** 8599 (2005)
77. M Imai, K Hashizaki, H Taguchi, Y Saito, S Motohashi *J. Colloid Interface Sci.* **403** 77 (2013)
78. F C MacKintosh, S A Safran, P A Pincus *Europhys. Lett.* **12** 697 (1990)
79. S Schmitt, F Lequeux *Langmuir* **14** 283 (1998)
80. R G Larson *The Structure and Rheology of Complex Fluids* (New York: Oxford University Press, 1999) Ch. 12
81. F Kern, F Lequeux, R Zana, S J Candau *Langmuir* **10** 1714 (1994)
82. J Narayanan, Manohar, F Kern, F Lequeux, S J Candau *Langmuir* **13** 5235 (1997)
83. T Odijk *J. Polym. Sci. B* **15** 477 (1977)
84. J Skolnick, M Fixman *Macromolecules* **10** 944 (1977)
85. F Lequeux *Curr. Opin. Colloid Interface Sci.* **1** 341 (1996)
86. V A Andreev, A I Victorov *J. Chem. Phys.* **132** 054902 (2010)
87. C Sommer, J S Pedersen, S U Egelhaaf, L Cannavacciuolo, J Kohlbrecher, P Schurtenberger *Langmuir* **18** 2495 (2002)
88. F Lequeux *Europhys. Lett.* **19** 675 (1992)
89. A Khatory, F Lequeux, F Kern, S J Candau *Langmuir* **9** 1456 (1993)
90. L Ambrosone, R Angelico, A Ceglie, U Olsson, G Palazzo *Langmuir* **17** 6822 (2001)
91. M E Helgeson, T K Hodgdon, E W Kaler, N J Wagner *J. Colloid Interface Sci.* **349** 1 (2010)
92. C J Pipe, N J Kim, P A Vasquez, L P Cook, G H McKinley *J. Rheol.* **54** 881 (2010)
93. G L Hunter, E R Weeks *Rep. Prog. Phys.* **75** 066501 (2012)
94. A Zaccone, H H Winter, M Siebenbürger, M Ballauff *J. Rheol.* **58** 1219 (2014)
95. Y Rahmani, K van der Vaart, B dan Dam, Z Hu, V Chikkadi, P Schall *Soft Matter* **8** 4264 (2012)
96. H Rehage, N Willenbacher *Curr. Opin. Colloid Interface Sci.* **16** 1 (2011)
97. S MacCarrone, G Brambilla, O Pravaz, A Duri, M Ciccotti, J M Fromental, E Pashkovski, A Lips, D Sessoms, V Trappe, L Cipelletti *Soft Matter* **6** 5514 (2010)
98. Y Caram, F Bautista, J E Puig, O Manero *Rheol. Acta* **46** 45 (2006)
99. J Delgado, R Castillo *J. Colloid Interface Sci.* **312** 481 (2007)
100. A Mütze, P Heunemann, P Fischer *J. Rheol.* **58** 1647 (2014)
101. J K G Dhont, W J Briels *Rheol. Acta* **47** 257 (2008)
102. F Bautista, V V A Fernández, E R Macías, J H Pérez-López, J I Escalante, J E Puig, O Manero *J. Non-Newton Fluid Mech.* **177 – 178** 89 (2012)

103. S Hackelbusch, T Rossow, P Van Assenbergh, S Seiffert *Macromolecules* **46** 6273 (2013)
104. T Vermonden, M J van Steenbergen, N A M Besseling, A T M Marcelis, W E Hennink, E J R Sudholter, M A C Stuart *J. Am. Chem. Soc.* **126** 15802 (2004)
105. P Kujawa, A Audibert-Hayet, J Selb, F Candau *Macromolecules* **39** 384 (2006)
106. T Uneyama, S Suzuki, H Watanabe *Phys. Rev. E* **86** 031802 (2012)
107. E J Regalado, J Selb, F Candau *Macromolecules* **32** 8580 (1999)
108. J Sprakel, E Bartscherer, G Hoffmann, M A C Stuart, J van der Gucht *Phys. Rev. E* **78** 040802 (2008)
109. J Sprakel, J van der Gucht, M A C Stuart, N A M Besseling *Phys. Rev. E* **77** 061502 (2008)
110. W C Yount, D M Loveless, S L Craig *J. Am. Chem. Soc.* **127** 14488 (2005)
111. M Rubinstein, A N Semenov *Macromolecules* **34** 1058 (2001)
112. F Tanaka *Polymer Physics. Application to Molecular Association and Thermoreversible Gelation* (Cambridge: Cambridge University Press, 2011)
113. T Indei *J. Chem. Phys.* **127** 144905 (2007)
114. T Indei, J I Takimoto *J. Chem. Phys.* **133** 194902 (2010)
115. T Lu, L Xia, X Wang, A Wang, T Zhang *Langmuir* **27** 9815 (2011)
116. N S M Yusof, M N Khan *Adv. Colloid Interface Sci.* **193** – **194** 12 (2013)
117. H Rehage, H Hoffmann *J. Phys. Chem.* **92** 4712 (1988)
118. C Oelschlaeger, P Suwita, N Willenbacher *Langmuir* **26** 7045 (2010)
119. L J Magid, Z Han, Z Li, P D Butler *Langmuir* **16** 149 (2000)
120. N Vlachy, B Jagoda-Cwiklik, R Vácha, D Touraud, P Jungwirth, W Kunz *Adv. Colloid Interface Sci.* **146** 42 (2009)
121. K D Collins, G W Neilson, J E Enderby *Biophys. Chem.* **128** 95 (2007)
122. L Moreira, A Firoozabadi *Langmuir* **26** 15177 (2010)
123. B Lukanov, A Firoozabadi *Langmuir* **30** 6373 (2014)
124. C Morita, Y Imura, T Ogawa, H Kurata, T Kawai *Langmuir* **29** 5450 (2013)
125. L Brinchi, R Germani, P Di Profio, L Marte, G Savelli, R Oda, D Berti *J. Colloid Interface Sci.* **346** 100 (2010)
126. R Kumar, A M Ketner, S R Raghavan *Langmuir* **26** 5405 (2010)
127. A V Shibaev, M V Tamm, V S Molchanov, A V Rogachev, A I Kuklin, E E Dormidontova, O E Philippova *Langmuir* **30** 3705 (2014)
128. H Shi, W Ge, H Oh, S M Pattison, J T Huggins, Y Talmon, D J Hart, S Raghavan, J L Zakin *Langmuir* **29** 102 (2013)
129. M Pereira, C R Leal, A J Parola, U M Scheven *Langmuir* **26** 16715 (2010)
130. K Tsuchiya, Y Orihara, Y Kondo, N Yoshino, T Ohkubo, H Sakai, M Abe *J. Am. Chem. Soc.* **126** 12282 (2004)
131. Z Chu, Y Feng *Chem. Commun.* **47** 7191 (2011)
132. Y Lin, Y Qiao, Y Yan, J Huang *Soft Matter* **5** 3047 (2009)
133. R Kumar, G C Kalur, L Ziserman, D Danino, S V Raghavan *Langmuir* **23** 12849 (2007)
134. R Dagani *Chem. Eng. News* **75** 26 (1997)
135. H Suzuki, A Kumagai *Biosens. Bioelectron.* **18** 1289 (2003)
136. S Avramiotis, V Papadimitriou, E Hatzara, V Bekiari, P Lianosand, A Xenakis *Langmuir* **23** 4438 (2007)
137. F B Bombelli, D Berti, F Pini, U Keiderling, P Baglioni *J. Phys. Chem. B* **108** 16427 (2004)
138. A Victorov, C Radke, J Prausnitz *Phys. Chem. Chem. Phys.* **8** 264 (2006)
139. A I Victorov *Fluid Phase Equilib.* **241** 334 (2006)
140. N Plotnikov, A I Victorov *Fluid Phase Equilib.* **261** 26 (2007)
141. A I Victorov *J. Chem. Eng. Data* **59** 2995 (2014)
142. A I Victorov, A Fredenslund, N A Smirnova *Fluid Phase Equilib.* **66** 187 (1991)
143. N Smirnova, A Victorov, in *Equations of State for Fluids and Fluid Mixtures* Vol. 1 (Eds J V Sengers, R F Kayser, C J Peters, H J White) (Amsterdam: Elsevier, 2000) p. 255
144. T Mehling, T Ingram, I Smirnova *Langmuir* **28** 118 (2012)
145. T Mehling, T Ingram, S Storm, U Bobe, F Liu, M Michel, I Smirnova *Colloids Surf., A* **431** 105 (2013)
146. E A Safonova, T Mehling, S Storm, E Ritter, I V Smirnova *Chem. Eng. Res. Des.* **92** 2840 (2014)